Table S3: VEO IBD Gene List: Genes Previously Reported to have a Causal Association with VEO IBD PMID:25058236

COL7A1
FERMT1
IKBKG
TTC7A
ADAM17
GUCY2C
CYBB
CYBA
NCF1
NCF2
NCF4
SLC37A4
G6PC3
ITGB2
MVK
PLCG2
MEFV
STXBP2
XIAP
SH2D1A
HPS1
HPS4
HPS6
ICOS
LRBA
IL21
BTK
PIK3R1
CD40LG
AICDA
WAS
DCLRE1C
ZAP70
RAG2
IL2RG
LIG4
ADA
CD3g
DKC1
RTEL1
DOCK8
FOXP3
IL2RA
STAT1
IL10RA
IL10RB
IL10
MASP2
SKIV2L
TTC37

Table S4: VEO Top Key Drivers

keydrivers	is_signature	hits	downstream	signature_in_	subnetwork_s	signature_in_	network_size	signature	optimal_laye	fold_change_	pvalue_whole	fold_change_	pvalue_subne	pvalue_corre	keydriver
NFAM1	1	201	615	664	7528	664	7528	665	6	3.70537761	6.13E-71	3.70537761	6.13E-71	4.62E-67	1
GBP5	1	145	395	664	7528	664	7528	665	5	4.1618118	5.19E-57	4.1618118	5.19E-57	3.90E-53	1
STAT1	1	31	31	664	7528	664	7528	665	2	11.3373494	1.07E-33	11.3373494	1.07E-33	8.03E-30	1
STX11	1	70	164	664	7528	664	7528	665	4	4.83911255	5.39E-32	4.83911255	5.39E-32	4.05E-28	1
ARHGDIB	1	154	671	664	7528	664	7528	665	8	2.60201462	7.61E-32	2.60201462	7.61E-32	5.73E-28	1
VAV1	1	30	34	664	7528	664	7528	665	3	10.0035436	4.16E-28	10.0035436	4.16E-28	3.13E-24	1
ARHGAP30	1	125	537	664	7528	664	7528	665	5	2.63904781	3.77E-26	2.63904781	3.77E-26	2.84E-22	1
CASZ1	1	24	25	664	7528	664	7528	665	3	10.8838554	7.69E-25	10.8838554	7.69E-25	5.79E-21	1
C1ORF228	1	30	39	664	7528	664	7528	665	5	8.721038	1.24E-24	8.721038	1.24E-24	9.33E-21	1
CYBB	1	22	22	664	7528	664	7528	665	2	11.3373494	4.59E-24	11.3373494	4.59E-24	3.45E-20	1
SLAMF8	1	26	30	664	7528	664	7528	665	3	9.82570281	4.74E-24	9.82570281	4.74E-24	3.57E-20	1
DRAM1	1	53	127	664	7528	664	7528	665	5	4.73133479	7.86E-24	4.73133479	7.86E-24	5.92E-20	1
SNX10	1	26	60	664	7528	664	7528	665	3	4.91285141	9.31E-13	4.91285141	9.31E-13	7.01E-09	1

Table S5:
IIBDGC GWAS ENRICHMENT In TRIM22 locus

0.01 cM:	chr	position	IBD: p-value	IBD: n_markers	CD: p-value	CD: n_markers	UC: p-value	UC: n_markers
TRIM22	11	5734619	0.08913	163	0.006027	157	0.03147	165
0.1 cM:	chr	position	IBD: p-value	IBD: n_markers	CD: p-value	CD: n_markers	UC: p-value	UC: n_markers
TRIM22	11	5734619	0.003694	332	0.006027	319	0.02398	337
1cM:	chr	position	IBD: p-value	IBD: n_markers	CD: p-value	CD: n_markers	UC: p-value	UC: n_markers
TRIM22	11	5734619	0.001465	5682	0.0003264	5640	0.0002493	5731

Table S6:
IIBDGC GWAS ENRICHMENT TRIM22 eQTL (NCBI) enrichment

	IBD	CD	UC
chr11:5077653	0.1452	0.4114	0.04264
chr11:5060791	0.1603	0.3978	0.04048
chr11:5059064	0.1559	0.4066	0.03872
chr11:5020799	0.3528	0.3084	0.07128
chr11:5020832	0.3478	0.3139	0.07045
chr11:5019217	0.3495	0.3058	0.07004
chr11:5019357	0.3503	0.3076	0.07054
chr11:5020189	0.3513	0.3084	0.07105
chr11:5020509	0.3538	0.3081	0.07163
chr11:5024139	0.346	0.317	0.07096
chr11:5073486	0.05608	0.5467	0.08671
chr11:5016553	0.4019	0.4234	0.1344
chr11:5719667	0.7601	0.657	0.5903

Table S7 Genes in eQTL Enriched Pathways

Enrichment analysis report

Enrichment by Pathway Maps

					WTCCC_IBD_GWAS_1e-3_union_NHGRI_IBD_UC_CD_blood_genelist				WTCCC_IBD_GWAS_1e-3_union_NHGRI_IBD_UC_CD_intestine_genelist			
#	Maps	Total	min(pValue)	Min FDR	p-value	FDR	In Data	Network Objects from Active Data	p-value	FDR	In Data	Network Objects from Active Data
1	Transcription_P53 signaling pathway	39	2.441E-04	4.171E-02	8.248E-02	3.406E-01	2	MKP-7, VEGF-A	2.441E-04	4.171E-02	3	VEGF-A, c-Fos, MKP-7
2	Signal transduction_PKA signaling	51	3.812E-04	1.403E-01	3.812E-04	1.403E-01	5	AKAP12, Adenylate cyclase, PP2A regulatory, DARPP-32, G-protein alpha-12 family	1.502E-01	1.783E-01	1	Adenylate cyclase
3	Immune response_C3a signaling	48	4.532E-04	4.171E-02	2.760E-03	1.410E-01	4	RhoA, Adenylate cyclase, CD40(TNFRSF5), VEGF-A	4.532E-04	4.171E-02	3	Adenylate cyclase, VEGF-A, CD40(TNFRSF5)
4	Immune response_Antiviral actions of Interferons	52	5.741E-04	4.171E-02	2.573E-02	2.192E-01	3	IRF1, MHC class I, HLA-A	5.741E-04	4.171E-02	3	CIITA, HLA-A, MHC class I
5	Immune response_HSP60 and HSP70/ TLR signaling pathway	54	6.416E-04	4.171E-02	4.240E-03	1.410E-01	4	TLR4, MHC class I, CD40(TNFRSF5), TPL2(MAP3K8)	6.416E-04	4.171E-02	3	HSP70, CD40(TNFRSF5), MHC class I
6	Regulation of CFTR activity (normal and CF)	62	9.436E-04	1.403E-01	9.436E-04	1.403E-01	5	Syk, Annexin V, Adenylate cyclase, COMMD1 (MURR1), PP2A regulatory	1.796E-01	1.938E-01	1	Adenylate cyclase
7	Neuroprotective action of lithium	63	1.008E-03	5.240E-02	1.808E-01	4.428E-01	2	VEGF-A, PP1-cat	1.008E-03	5.240E-02	3	VEGF-A, HSP70, WNT
8	Immune response_PGE2 signaling in immune response	45	2.173E-03	1.410E-01	2.173E-03	1.410E-01	4	Adenylate cyclase, IL-2, CREM (activators), CREM (repressors)	1.337E-01	1.783E-01	1	Adenylate cyclase
9	Proteolysis_Putative ubiquitin pathway	23	2.366E-03	7.636E-02	2.475E-01	5.017E-01	1	UBCH7	2.366E-03	7.636E-02	2	HSP70, UBCH7
10	Proteolysis_Role of Parkin in the Ubiquitin-Proteasomal Pathway	24	2.576E-03	7.636E-02	2.567E-01	5.112E-01	1	UBCH7	2.576E-03	7.636E-02	2	HSP70, UBCH7

Table S8 Crohn's GWAS Enriched Blood eQTL Overlap with the VEO Network

snp	snp_chr	snp_pos_hg1	gene	ensembl_id	gene_symbol	cis_trans_ind	fdr	pvalue	tissue	IBD_META_P
rs1872691	16	50350210		ENSG000001	ADCY7	cis	0	0	Blood	5.59E-18
rs3813755	16	50348577		ENSG000001	ADCY7	cis	0	0	Blood	7.89E-18
rs3826173	16	50345012		ENSG000001	ADCY7	cis	0	0	Blood	1.88E-17
rs4785210	16	50340154		ENSG000001	ADCY7	cis	0	0	Blood	3.44E-11
rs4785403	16	50340217		ENSG000001	ADCY7	cis	0	0	Blood	3.42E-11
rs4785412	16	50385468		ENSG000001	ADCY7	cis	0	0	Blood	1.12E-17
rs7184802	16	50355996		ENSG000001	ADCY7	cis	0	0	Blood	7.30E-18
rs8047812	16	50389485		ENSG000001	ADCY7	cis	0	0	Blood	1.04E-19
rs4643314	16	50375955		ENSG000001	ADCY7	cis	0	1.00E-13	Blood	1.11E-20
rs12325247	16	50363559		ENSG000001	ADCY7	cis	0	1.03E-13	Blood	5.90E-21
rs9525625	13	43018030		ENSG00000(	AKAP11	cis	0	1.06E-06	Blood	1.00E-10
rs3116494	2	204592021		ENSG000001	CD28	cis	0	6.11E-14	Blood	1.00E-10
rs1569723	20	44742064		LRG_40	CD40	cis	0	0	Blood	6.55E-11
rs2425752	20	44702120		LRG_40	CD40	cis	0	0	Blood	3.09E-08
rs4810485	20	44747947		LRG_40	CD40	cis	0	0	Blood	3.89E-10
rs6131010	20	44724305		LRG_40	CD40	cis	0	0	Blood	3.89E-08
rs12624433	20	44680853		LRG_40	CD40	cis	0	2.00E-20	Blood	3.69E-09
rs1569723	20	44742064		LRG_40	CD40	cis	0.03	6.13E-05	Blood	6.55E-11
rs11230556	11	60765984	ENSG00000(	ENSG00000(	CD6	Cis	0.1	1.46E-06	Blood	6.43E-07
rs11230555	11	60763134	ENSG00000(	ENSG00000(	CD6	Cis	0.1	1.86E-06	Blood	8.19E-07
rs12421176	11	60805385	ENSG00000(	ENSG00000(	CD6	Cis	0.1	3.39E-06	Blood	4.70E-07
rs12293191	11	60806747	ENSG00000(	ENSG00000(	CD6	Cis	0.1	3.51E-06	Blood	3.95E-07
rs11230556	11	60765984	ENSG00000(	ENSG00000(	CD6	Cis	0.1	9.63E-06	Blood	6.43E-07
rs11085735	19	10602180		ENSG000001	CDKN2D	cis	0.01	1.48E-05	Blood	1.36E-10
rs913678	20	48955424		ENSG000001	CEBPB	cis	0	8.55E-18	Blood	4.59E-08
rs1199096	10	59950234		ENSG000001	CISD1	Cis	NA	0	Whole blood	5.78E-07
rs1199096	10	59950234		ENSG000001	CISD1	Cis	NA	0	Whole blood	5.78E-07
rs1199096	10	59950234		ENSG000001	CISD1	Cis	NA	0	Whole blood	5.78E-07
rs1199096	10	59950234		ENSG000001	CISD1	cis	0	0	Blood	5.78E-07
rs1199103	10	59947231		ENSG000001	CISD1	cis	0	0	Blood	1.88E-07

rs1416764	10	60040351		ENSG00000120	CISD1	cis		0	0	Blood	2.56E-07
rs1698402	10	59936444		ENSG00000120	CISD1	cis		0	0	Blood	2.57E-07
rs1769044	10	59958956		ENSG00000120	CISD1	cis		0	0	Blood	4.54E-07
rs1867571	10	60038850		ENSG00000120	CISD1	cis		0	0	Blood	3.00E-07
rs1867573	10	60042972		ENSG00000120	CISD1	cis		0	0	Blood	3.55E-07
rs2153281	10	59972453		ENSG00000120	CISD1	cis		0	0	Blood	2.71E-07
rs2251039	10	60028894		ENSG00000120	CISD1	cis		0	0	Blood	2.46E-07
rs2253192	10	59999323		ENSG00000120	CISD1	cis		0	0	Blood	1.93E-07
rs2254775	10	60036815		ENSG00000120	CISD1	cis		0	0	Blood	2.20E-07
rs2486491	10	59970391		ENSG00000120	CISD1	cis		0	0	Blood	2.97E-07
rs2590307	10	59977161		ENSG00000120	CISD1	cis		0	0	Blood	5.12E-07
rs2590313	10	59986383		ENSG00000120	CISD1	cis		0	0	Blood	3.31E-07
rs2590339	10	60012231		ENSG00000120	CISD1	cis		0	0	Blood	2.78E-07
rs2790155	10	59974744		ENSG00000120	CISD1	cis		0	0	Blood	2.92E-07
rs2790170	10	60028507		ENSG00000120	CISD1	cis		0	0	Blood	1.87E-07
rs2790179	10	60035372		ENSG00000120	CISD1	Cis	NA		0	Whole blood	2.38E-07
rs2790179	10	60035372		ENSG00000120	CISD1	Cis	NA		0	Whole blood	2.38E-07
rs2790179	10	60035372		ENSG00000120	CISD1	Cis	NA		0	Whole blood	2.38E-07
rs2790179	10	60035372		ENSG00000120	CISD1	cis		0	0	Blood	2.38E-07
rs2790182	10	60039877		ENSG00000120	CISD1	cis		0	0	Blood	2.25E-07
rs2790189	10	60042576		ENSG00000120	CISD1	cis		0	0	Blood	1.09E-07
rs2790216	10	59997926		ENSG00000120	CISD1	cis		0	0	Blood	1.60E-07
rs2790236	10	59985102		ENSG00000120	CISD1	cis		0	0	Blood	2.79E-07
rs2790241	10	60015313		ENSG00000120	CISD1	cis		0	0	Blood	2.28E-07
rs2790242	10	59980652		ENSG00000120	CISD1	cis		0	0	Blood	5.78E-07
rs1199096	10	59950234	ENSG00000120	ENSG00000120	CISD1	Cis		0.1	2.81E-18	Blood	5.78E-07
rs1199103	10	59947231	ENSG00000120	ENSG00000120	CISD1	Cis		0.1	2.91E-18	Blood	1.88E-07
rs2486491	10	59970391	ENSG00000120	ENSG00000120	CISD1	Cis		0.1	3.03E-18	Blood	2.97E-07
rs2153281	10	59972453	ENSG00000120	ENSG00000120	CISD1	Cis		0.1	3.05E-18	Blood	2.71E-07
rs1769044	10	59958956	ENSG00000120	ENSG00000120	CISD1	Cis		0.1	3.07E-18	Blood	4.54E-07
rs2790242	10	59980652	ENSG00000120	ENSG00000120	CISD1	Cis		0.1	3.09E-18	Blood	5.78E-07
rs2790155	10	59974744	ENSG00000120	ENSG00000120	CISD1	Cis		0.1	3.11E-18	Blood	2.92E-07

rs2590313	10	59986383	ENSG00000	ENSG00000	CISD1	Cis	0.1	3.15E-18	Blood	3.31E-07
rs2790236	10	59985102	ENSG00000	ENSG00000	CISD1	Cis	0.1	3.16E-18	Blood	2.79E-07
rs2790216	10	59997926	ENSG00000	ENSG00000	CISD1	Cis	0.1	4.26E-18	Blood	1.60E-07
rs1698402	10	59936444	ENSG00000	ENSG00000	CISD1	Cis	0.1	4.34E-18	Blood	2.57E-07
rs2590307	10	59977161	ENSG00000	ENSG00000	CISD1	Cis	0.1	4.78E-18	Blood	5.12E-07
rs2253192	10	59999323	ENSG00000	ENSG00000	CISD1	Cis	0.1	5.19E-18	Blood	1.93E-07
rs2590339	10	60012231	ENSG00000	ENSG00000	CISD1	Cis	0.1	1.28E-17	Blood	2.78E-07
rs2790189	10	60042576	ENSG00000	ENSG00000	CISD1	Cis	0.1	1.87E-17	Blood	1.09E-07
rs2790170	10	60028507	ENSG00000	ENSG00000	CISD1	Cis	0.1	2.02E-17	Blood	1.87E-07
rs2251039	10	60028894	ENSG00000	ENSG00000	CISD1	Cis	0.1	2.19E-17	Blood	2.46E-07
rs1867571	10	60038850	ENSG00000	ENSG00000	CISD1	Cis	0.1	2.41E-17	Blood	3.00E-07
rs2790179	10	60035372	ENSG00000	ENSG00000	CISD1	Cis	0.1	2.60E-17	Blood	2.38E-07
rs2254775	10	60036815	ENSG00000	ENSG00000	CISD1	Cis	0.1	2.63E-17	Blood	2.20E-07
rs1416764	10	60040351	ENSG00000	ENSG00000	CISD1	Cis	0.1	2.88E-17	Blood	2.56E-07
rs1867573	10	60042972	ENSG00000	ENSG00000	CISD1	Cis	0.1	3.01E-17	Blood	3.55E-07
rs1416763	10	60029163	ENSG00000	ENSG00000	CISD1	Cis	0.1	4.00E-17	Blood	1.80E-07
rs2790182	10	60039877	ENSG00000	ENSG00000	CISD1	Cis	0.1	4.05E-17	Blood	2.25E-07
rs2790241	10	60015313	ENSG00000	ENSG00000	CISD1	Cis	0.1	5.42E-17	Blood	2.28E-07
rs740495	19	1124835		ENSG00000	CNN2	cis	0	1.06E-06	Blood	1.20E-14
rs2472649	4	74857708		ENSG00000	CXCL5	cis	0	0	Blood	4.15E-07
rs7512140	1	161463601		ENSG00000	FCGR2B	cis	0	0	Blood	5.90E-07
rs7103915	11	63944370		LRG_180	FERMT3	cis	0.01	1.39E-05	Blood	9.57E-09
rs11231713	11	63931849		LRG_180	FERMT3	cis	0.02	3.75E-05	Blood	5.27E-09
rs2096706	11	63924446		LRG_180	FERMT3	cis	0.02	4.46E-05	Blood	1.32E-08
rs11601686	11	64189110		LRG_180	FERMT3	cis	0.02	4.83E-05	Blood	1.19E-08
rs947939	11	63885287		LRG_180	FERMT3	cis	0.03	6.18E-05	Blood	2.54E-08
rs1205843	20	30742996		ENSG00000	HCK	cis	0	1.06E-05	Blood	9.38E-07
rs7911264	10	94436851		ENSG00000	HHEX	cis	0	1.50E-19	Blood	2.98E-08
rs2497306	10	94485211		ENSG00000	HHEX	cis	0	2.93E-15	Blood	7.38E-08
rs2497304	10	94492716		ENSG00000	HHEX	cis	0	6.22E-15	Blood	6.26E-08
rs10882091	10	94374377		ENSG00000	HHEX	cis	0	2.76E-14	Blood	1.01E-07
rs6583830	10	94398118		ENSG00000	HHEX	cis	0	4.64E-14	Blood	8.86E-08

rs7914814	10	94382950	ENSG00000178HHEX	cis		0	4.64E-14	Blood	8.66E-08
rs947591	10	94495753	ENSG00000178HHEX	cis		0	1.03E-12	Blood	1.06E-07
rs12778642	10	94464307	ENSG00000178HHEX	cis		0	2.32E-11	Blood	3.67E-08
rs5015480	10	94465559	ENSG00000178HHEX	cis		0	3.31E-08	Blood	3.29E-07
rs7924271	10	94542446	ENSG00000178HHEX	cis		0.02	5.96E-05	Blood	7.07E-07
rs1007654	17	38111354	ENSG00000161IKZF3	cis		0	0	Blood	2.80E-12
rs11869286	17	37813856	ENSG00000161IKZF3	cis		0	0	Blood	1.80E-09
rs1476278	17	37836243	ENSG00000161IKZF3	cis		0	0	Blood	2.60E-12
rs1877031	17	37814080	ENSG00000161IKZF3	cis		0	0	Blood	1.84E-09
rs2271308	17	37817482	ENSG00000161IKZF3	cis		0	0	Blood	1.33E-07
rs2517955	17	37843681	ENSG00000161IKZF3	cis		0	0	Blood	3.66E-13
rs8065126	17	38099035	ENSG00000161IKZF3	cis		0	0	Blood	3.36E-13
s903502	17	37829604	ENSG00000161IKZF3	cis		0	0	Blood	5.21E-15
rs9303274	17	37836353	ENSG00000161IKZF3	cis		0	0	Blood	2.24E-12
rs9303277	17	37976469	ENSG00000161IKZF3	Cis	NA		0	Whole blood	7.90E-28
rs9303277	17	37976469	ENSG00000161IKZF3	Cis	NA		0	Whole blood	7.90E-28
rs9303277	17	37976469	ENSG00000161IKZF3	Cis	NA		0	Whole blood	7.90E-28
rs3859192	17	38128648	ENSG00000161IKZF3	cis		0	4.41E-16	Blood	2.38E-14
rs12453334	17	38153473	ENSG00000161IKZF3	cis		0	2.28E-13	Blood	5.25E-09
rs2227319	17	38170845	ENSG00000161IKZF3	cis		0	3.49E-13	Blood	5.01E-09
rs907091	17	37921742	ENSG00000161IKZF3	cis		0	3.39E-12	Blood	4.87E-29
rs8077456	17	38128765	ENSG00000161IKZF3	cis		0	1.32E-11	Blood	5.30E-07
rs10445308	17	37938047	ENSG00000161IKZF3	cis		0	2.53E-11	Blood	6.67E-36
rs907092	17	37922259	ENSG00000161IKZF3	cis		0	6.65E-11	Blood	1.77E-37
rs8075668	17	38137623	ENSG00000161IKZF3	cis		0	2.98E-08	Blood	6.32E-11
rs6503525	17	38095174	ENSG00000161IKZF3	cis		0	4.14E-06	Blood	2.66E-15
rs8079416	17	38092713	ENSG00000161IKZF3	cis		0	5.04E-06	Blood	2.71E-15
rs7212938	17	38122680	ENSG00000161IKZF3	cis		0	6.90E-06	Blood	1.07E-13
rs1008723	17	38066267	ENSG00000161IKZF3	cis		0.01	1.89E-05	Blood	1.18E-25
rs869402	17	38068043	ENSG00000161IKZF3	cis		0.01	1.97E-05	Blood	8.09E-24
rs2305479	17	38062217	ENSG00000161IKZF3	cis		0.01	1.99E-05	Blood	1.34E-29
rs3816470	17	37985801	ENSG00000161IKZF3	cis		0.01	2.32E-05	Blood	4.69E-27

rs7224129	17	38075426	ENSG00000172IKZF3	cis	0.02	3.60E-05	Blood	4.74E-24
rs7219923	17	38074518	ENSG00000172IKZF3	cis	0.02	3.72E-05	Blood	6.98E-24
rs9303281	17	38074046	ENSG00000172IKZF3	cis	0.02	3.78E-05	Blood	5.34E-24
rs9901146	17	38043343	ENSG00000172IKZF3	cis	0.02	3.82E-05	Blood	1.74E-29
rs907091	17	37921742	ENSG00000172IKZF3	cis	0.02	3.92E-05	Blood	4.87E-29
rs9303277	17	37976469	ENSG00000172IKZF3	cis	0.02	5.35E-05	Blood	7.90E-28
rs8070454	17	38160754	ENSG00000172IKZF3	cis	0.03	6.08E-05	Blood	4.05E-10
rs8078723	17	38166879	ENSG00000172IKZF3	cis	0.03	6.88E-05	Blood	3.62E-10
rs2070729	5	131819921	ENSG00000172IRF1	cis	0	4.51E-10	Blood	7.57E-23
rs10077785	5	131801158	ENSG00000172IRF1	cis	0	4.58E-09	Blood	6.64E-19
rs10039559	5	131804507	ENSG00000172IRF1	cis	0	4.66E-09	Blood	6.95E-18
rs2248116	5	131804347	ENSG00000172IRF1	cis	0	5.18E-09	Blood	1.77E-37
rs2522057	5	131801947	ENSG00000172IRF1	cis	0	7.83E-09	Blood	4.61E-37
rs2188962	5	131770805	ENSG00000172IRF1	cis	0	8.50E-09	Blood	3.74E-37
rs11745587	5	131796922	ENSG00000172IRF1	cis	0	9.96E-09	Blood	4.27E-29
rs12521868	5	131784393	ENSG00000172IRF1	cis	0	1.23E-08	Blood	3.05E-37
rs3857440	5	131794069	ENSG00000172IRF1	cis	0	1.66E-08	Blood	1.99E-18
rs2548993	5	131808869	ENSG00000172IRF1	cis	0	2.10E-08	Blood	3.84E-19
rs11748193	5	131725329	ENSG00000172IRF1	cis	0	3.24E-08	Blood	7.93E-36
rs11746555	5	131727033	ENSG00000172IRF1	cis	0	3.41E-08	Blood	5.24E-36
rs4540166	5	131779857	ENSG00000172IRF1	cis	0	3.50E-08	Blood	2.74E-19
rs11744116	5	131779760	ENSG00000172IRF1	cis	0	3.51E-08	Blood	1.31E-19
rs11739135	5	131733397	ENSG00000172IRF1	cis	0	4.07E-08	Blood	4.50E-36
rs4235801	5	131782444	ENSG00000172IRF1	cis	0	6.04E-08	Blood	4.30E-19
rs17622208	5	131717050	ENSG00000172IRF1	cis	0	3.43E-07	Blood	1.69E-25
rs11950562	5	131652529	ENSG00000172IRF1	cis	0	3.58E-07	Blood	7.94E-25
rs10058074	5	131686146	ENSG00000172IRF1	cis	0	5.12E-07	Blood	1.72E-25
rs4705938	5	131694077	ENSG00000172IRF1	cis	0	5.41E-07	Blood	1.82E-25
rs10071051	5	131752620	ENSG00000172IRF1	cis	0	7.87E-07	Blood	1.31E-15
rs17622656	5	131820997	ENSG00000172IRF1	cis	0	8.81E-07	Blood	3.10E-37
rs2285673	5	131755969	ENSG00000172IRF1	cis	0	1.06E-06	Blood	5.66E-16
rs17715481	5	131815384	ENSG00000172IRF1	cis	0	5.80E-06	Blood	5.41E-09

rs7705189	5	131623358	ENSG000001	IRF1	cis	0.01	1.15E-05	Blood	7.89E-17
rs2089855	5	131573529	ENSG000001	IRF1	cis	0.03	8.77E-05	Blood	2.17E-20
rs7701414	5	131585958	ENSG000001	IRF1	cis	0.04	9.12E-05	Blood	7.08E-20
rs4594848	5	131586598	ENSG000001	IRF1	cis	0.04	9.61E-05	Blood	6.65E-20
rs10758677	9	5188078	ENSG00000(	JAK2	cis	0	0	Blood	2.10E-14
rs10815144	9	5010192	ENSG00000(	JAK2	cis	0	0	Blood	9.17E-17
rs1328917	9	5049065	ENSG00000(	JAK2	cis	0	0	Blood	6.31E-18
rs2149556	9	5059440	ENSG00000(	JAK2	cis	0	0	Blood	2.42E-15
rs2230724	9	5081780	ENSG00000(	JAK2	cis	0	0	Blood	5.57E-17
rs7023146	9	5040163	ENSG00000(	JAK2	cis	0	0	Blood	4.64E-18
rs7847294	9	5097281	ENSG00000(	JAK2	cis	0	0	Blood	1.18E-14
rs7861755	9	5273180	ENSG00000(	JAK2	cis	0	0	Blood	1.25E-09
rs7034753	9	5021514	ENSG00000(	JAK2	cis	0	4.00E-20	Blood	4.86E-14
rs7850484	9	5147817	ENSG00000(	JAK2	cis	0	6.90E-19	Blood	1.27E-26
rs11793659	9	5109707	ENSG00000(	JAK2	cis	0	3.90E-18	Blood	3.34E-27
rs17425637	9	5110000	ENSG00000(	JAK2	cis	0	3.90E-18	Blood	4.86E-28
rs10815157	9	5108771	ENSG00000(	JAK2	cis	0	4.19E-18	Blood	8.07E-27
rs3824433	9	5113577	ENSG00000(	JAK2	cis	0	5.15E-18	Blood	4.62E-27
rs3780374	9	5099677	ENSG00000(	JAK2	cis	0	5.39E-18	Blood	1.03E-27
rs17425819	9	5114773	ENSG00000(	JAK2	cis	0	5.48E-18	Blood	5.42E-28
rs3780373	9	5098223	ENSG00000(	JAK2	cis	0	7.61E-18	Blood	3.00E-26
rs7047795	9	5181467	ENSG00000(	JAK2	cis	0	9.65E-18	Blood	9.30E-26
rs10119004	9	5071049	ENSG00000(	JAK2	cis	0	9.84E-18	Blood	9.93E-17
rs3780381	9	5114523	ENSG00000(	JAK2	cis	0	1.52E-17	Blood	8.73E-28
rs7038687	9	5134065	ENSG00000(	JAK2	cis	0	2.48E-17	Blood	1.07E-26
rs10121316	9	5147539	ENSG00000(	JAK2	cis	0	2.54E-17	Blood	1.32E-26
rs10758674	9	5163645	ENSG00000(	JAK2	cis	0	2.57E-17	Blood	3.16E-26
rs7029084	9	5174638	ENSG00000(	JAK2	cis	0	2.58E-17	Blood	5.71E-26
rs7871515	9	5175288	ENSG00000(	JAK2	cis	0	2.76E-17	Blood	7.51E-26
rs7040922	9	5174829	ENSG00000(	JAK2	cis	0	3.00E-17	Blood	1.47E-25
rs3780382	9	5232299	ENSG00000(	JAK2	cis	0	3.21E-17	Blood	2.38E-22
rs16922779	9	5200127	ENSG00000(	JAK2	cis	0	3.25E-17	Blood	6.92E-23

rs10491650	9	5203054	ENSG00000(	JAK2	cis	0	3.47E-17	Blood	3.56E-22
rs12343038	9	5178579	ENSG00000(	JAK2	cis	0	3.61E-17	Blood	7.37E-26
rs10491651	9	5200060	ENSG00000(	JAK2	cis	0	3.64E-17	Blood	2.27E-23
rs16922786	9	5200714	ENSG00000(	JAK2	cis	0	3.64E-17	Blood	3.58E-23
rs6476948	9	5204404	ENSG00000(	JAK2	cis	0	3.84E-17	Blood	5.25E-23
rs10974993	9	5182159	ENSG00000(	JAK2	cis	0	4.00E-17	Blood	3.77E-26
rs10122037	9	5192874	ENSG00000(	JAK2	cis	0	4.69E-17	Blood	2.48E-24
rs1322222	9	5190444	ENSG00000(	JAK2	cis	0	4.74E-17	Blood	1.56E-23
rs10118930	9	5148278	ENSG00000(	JAK2	cis	0	4.80E-17	Blood	4.57E-27
rs7850294	9	5191128	ENSG00000(	JAK2	cis	0	4.97E-17	Blood	1.51E-22
rs12115301	9	5180548	ENSG00000(	JAK2	cis	0	5.74E-17	Blood	7.05E-26
rs2146040	9	5260039	ENSG00000(	JAK2	cis	0	6.34E-17	Blood	1.35E-21
rs7870536	9	5245493	ENSG00000(	JAK2	cis	0	6.46E-17	Blood	9.41E-23
rs10283467	9	5244356	ENSG00000(	JAK2	cis	0	6.55E-17	Blood	2.10E-23
rs7850228	9	5210671	ENSG00000(	JAK2	cis	0	9.97E-17	Blood	6.59E-19
rs12347727	9	5000811	ENSG00000(	JAK2	cis	0	2.75E-16	Blood	1.01E-35
rs3780367	9	5068755	ENSG00000(	JAK2	cis	0	2.76E-16	Blood	4.36E-34
rs7859390	9	5062473	ENSG00000(	JAK2	cis	0	2.99E-16	Blood	5.16E-34
rs7862042	9	5268139	ENSG00000(	JAK2	cis	0	3.05E-16	Blood	1.79E-19
rs7851556	9	5022807	ENSG00000(	JAK2	cis	0	3.37E-16	Blood	4.87E-34
rs2149555	9	5053743	ENSG00000(	JAK2	cis	0	3.75E-16	Blood	2.46E-34
rs10121491	9	5046935	ENSG00000(	JAK2	cis	0	3.76E-16	Blood	1.70E-33
rs7036761	9	5198781	ENSG00000(	JAK2	cis	0	4.95E-16	Blood	4.14E-19
rs10815149	9	5063701	ENSG00000(	JAK2	cis	0	5.23E-16	Blood	8.97E-33
rs10974944	9	5070831	ENSG00000(	JAK2	cis	0	7.01E-16	Blood	4.66E-34
rs3780366	9	5068596	ENSG00000(	JAK2	cis	0	8.17E-16	Blood	4.74E-34
rs11999802	9	5189773	ENSG00000(	JAK2	cis	0	1.22E-15	Blood	2.75E-17
rs10974914	9	5014332	ENSG00000(	JAK2	cis	0	1.54E-15	Blood	5.23E-33
rs7030260	9	5008070	ENSG00000(	JAK2	cis	0	2.96E-15	Blood	8.00E-33
rs4425810	9	5222208	ENSG00000(	JAK2	cis	0	3.12E-15	Blood	7.89E-21
rs4142064	9	5221818	ENSG00000(	JAK2	cis	0	3.48E-15	Blood	6.75E-21
rs10975003	9	5213687	ENSG00000(	JAK2	cis	0	5.21E-15	Blood	2.05E-16

rs2224571	9	5196253		ENSG00000(	JAK2	cis		0	7.69E-15	Blood	4.20E-23
rs7034878	9	5058991		ENSG00000(	JAK2	Cis	NA		2.42E-12	Whole blood	1.36E-15
rs7034878	9	5058991		ENSG00000(	JAK2	Cis	NA		9.36E-12	Whole blood	1.36E-15
rs7849191	9	4988761		ENSG00000(	JAK2	cis		0	2.24E-11	Blood	5.31E-24
rs10974892	9	4964774		ENSG00000(	JAK2	cis		0	2.72E-11	Blood	1.89E-16
rs10758669	9	4981602		ENSG00000(	JAK2	cis		0	4.83E-11	Blood	7.88E-45
rs1536800	9	5055434		ENSG00000(	JAK2	cis		0	7.95E-11	Blood	3.31E-31
rs7034878	9	5058991		ENSG00000(	JAK2	Cis	NA		8.67E-08	Whole blood	1.36E-15
rs10758677	9	5188078	---	ENSG00000(	JAK2	Cis		0.1	9.51E-08	Blood	2.10E-14
rs7847294	9	5097281	---	ENSG00000(	JAK2	Cis		0.1	1.42E-07	Blood	1.18E-14
rs2230724	9	5081780	---	ENSG00000(	JAK2	Cis		0.1	2.26E-07	Blood	5.57E-17
rs7032169	9	4966178		ENSG00000(	JAK2	cis		0.01	1.23E-05	Blood	5.82E-15
rs11041476	11	1875067		ENSG00000	LSP1	Cis	NA		1.11E-12	Whole blood	3.28E-10
rs11041476	11	1875067		ENSG00000	LSP1	Cis	NA		5.63E-09	Whole blood	3.28E-10
rs11041476	11	1875067		ENSG00000	LSP1	Cis	NA		3.56E-05	Whole blood	3.28E-10
rs10908812	1	160879316		ENSG00000	LY9	cis		0	0	Blood	6.76E-07
rs11265510	1	160859559		ENSG00000	LY9	cis		0	0	Blood	7.76E-07
rs1333062	1	160846284		ENSG00000	LY9	cis		0	0	Blood	2.58E-08
rs2039415	1	160854445		ENSG00000	LY9	cis		0	0	Blood	1.02E-08
rs3820094	1	160849082		ENSG00000	LY9	cis		0	0	Blood	2.35E-08
rs4656956	1	160847617		ENSG00000	LY9	cis		0	0	Blood	2.21E-08
rs4656957	1	160850280		ENSG00000	LY9	cis		0	0	Blood	2.91E-08
rs7411035	1	160856076		ENSG00000	LY9	cis		0	0	Blood	2.94E-08
rs10763790	10	30791355		ENSG00000	MAP3K8	cis		0	0	Blood	9.05E-07
rs2771242	10	30762973		ENSG00000	MAP3K8	cis		0	1.58E-18	Blood	9.95E-08
rs593400	10	30762088		ENSG00000	MAP3K8	cis		0	1.74E-18	Blood	7.18E-08
rs619864	10	30750950		ENSG00000	MAP3K8	cis		0	3.14E-18	Blood	9.27E-08
rs603072	10	30755778		ENSG00000	MAP3K8	cis		0	3.36E-18	Blood	4.80E-08
rs598672	10	30742388		ENSG00000	MAP3K8	cis		0	3.85E-18	Blood	1.32E-07
rs602097	10	30747546		ENSG00000	MAP3K8	cis		0	4.73E-18	Blood	1.56E-07
rs602966	10	30755853		ENSG00000	MAP3K8	cis		0	6.27E-18	Blood	7.16E-08
rs10826797	10	30690376		ENSG00000	MAP3K8	cis		0	7.43E-16	Blood	7.91E-08

rs303428	10	30739058	ENSG00000	MAP3K8	cis		0	5.17E-15	Blood	3.27E-08
rs10763790	10	30791355	ENSG00000	MAP3K8	Cis	NA		7.11E-13	Whole blood	9.05E-07
rs2265186	10	30691743	ENSG00000	MAP3K8	cis		0	2.00E-12	Blood	7.04E-10
rs6481677	10	30701816	ENSG00000	MAP3K8	cis		0	2.54E-12	Blood	7.69E-10
rs1543725	10	30698873	ENSG00000	MAP3K8	cis		0	2.65E-12	Blood	5.02E-10
rs2480277	10	30703513	ENSG00000	MAP3K8	cis		0	2.84E-12	Blood	9.69E-10
rs1042058	10	30728101	ENSG00000	MAP3K8	cis		0	3.48E-12	Blood	2.10E-10
rs303436	10	30731893	ENSG00000	MAP3K8	cis		0	7.47E-12	Blood	1.64E-08
rs694346	10	30711929	ENSG00000	MAP3K8	cis		0	1.73E-11	Blood	5.60E-08
rs1536833	10	30699265	ENSG00000	MAP3K8	cis		0	2.13E-11	Blood	1.53E-07
rs10763790	10	30791355	ENSG00000	MAP3K8	Cis	NA		8.58E-09	Whole blood	9.05E-07
rs306583	10	30710057	ENSG00000	MAP3K8	cis		0	9.76E-09	Blood	6.07E-09
rs10763790	10	30791355	ENSG00000	MAP3K8	Cis	NA		7.46E-08	Whole blood	9.05E-07
rs2072711	22	37268555	LRG_159	NCF4	cis		0	0	Blood	1.00E-10
rs2072711	22	37268555	LRG_159	NCF4	cis		0	1.50E-18	Blood	1.00E-10
rs2072711	22	37268555	LRG_159	NCF4	cis		0	1.67E-10	Blood	1.00E-10
rs11660128	18	77227950	ENSG00000	NFATC1	cis		0	0	Blood	2.31E-07
rs11664153	18	77195813	ENSG00000	NFATC1	cis		0	0	Blood	3.10E-07
rs11664725	18	77192116	ENSG00000	NFATC1	cis		0	0	Blood	5.06E-08
rs3786185	18	77199023	ENSG00000	NFATC1	cis		0	0	Blood	7.24E-08
rs7236492	18	77220616	ENSG00000	NFATC1	cis		0	0	Blood	1.00E-10
rs7236492	18	77220616	ENSG00000	NFATC1	cis		0	0	Blood	3.05E-07
rs3786185	18	77199023	ENSG00000	NFATC1	cis		0.01	1.94E-05	Blood	7.24E-08
rs11664725	18	77192116	ENSG00000	NFATC1	cis		0.01	2.33E-05	Blood	5.06E-08
rs10521209	16	50755709	LRG_177	NOD2	cis		0	0	Blood	7.96E-22
rs1077861	16	50759547	LRG_177	NOD2	cis		0	0	Blood	5.32E-11
rs1109863	16	50692364	LRG_177	NOD2	cis		0	0	Blood	7.05E-15
rs11640716	16	50665089	LRG_177	NOD2	cis		0	0	Blood	2.80E-14
rs11647841	16	50743331	LRG_177	NOD2	cis		0	0	Blood	7.76E-24
rs12913	16	50668426	LRG_177	NOD2	cis		0	0	Blood	2.52E-14
rs12925755	16	50846162	LRG_177	NOD2	cis		0	0	Blood	1.06E-17
rs1420872	16	50807779	LRG_177	NOD2	cis		0	0	Blood	5.62E-24

rs1558663	16	50662844	LRG_177	NOD2	cis	0	0	Blood	2.63E-14
rs17221417	16	50739582	LRG_177	NOD2	cis	0	0	Blood	1.45E-51
rs17313265	16	50747704	LRG_177	NOD2	cis	0	0	Blood	1.64E-57
rs17314544	16	50820078	LRG_177	NOD2	cis	0	0	Blood	2.60E-25
rs1861758	16	50751787	LRG_177	NOD2	cis	0	0	Blood	2.57E-21
rs1861759	16	50745583	LRG_177	NOD2	cis	0	0	Blood	1.79E-20
rs2066843	16	50745199	LRG_177	NOD2	cis	0	0	Blood	2.14E-57
rs2066849	16	50687015	LRG_177	NOD2	cis	0	0	Blood	1.91E-15
rs2076756	16	50756881	LRG_177	NOD2	cis	0	0	Blood	2.83E-62
rs2111234	16	50734033	LRG_177	NOD2	cis	0	0	Blood	3.86E-08
rs2111435	16	50819910	LRG_177	NOD2	cis	0	0	Blood	4.10E-16
rs3135500	16	50766886	LRG_177	NOD2	cis	0	0	Blood	3.72E-21
rs3785142	16	50787147	LRG_177	NOD2	cis	0	0	Blood	2.51E-16
rs4486887	16	50677571	LRG_177	NOD2	cis	0	0	Blood	1.92E-15
rs4785224	16	50730446	LRG_177	NOD2	cis	0	0	Blood	6.59E-23
rs4785227	16	50842197	LRG_177	NOD2	cis	0	0	Blood	4.66E-15
rs4785450	16	50792268	LRG_177	NOD2	cis	0	0	Blood	3.67E-20
rs4785452	16	50842077	LRG_177	NOD2	cis	0	0	Blood	4.66E-15
rs5743266	16	50731096	LRG_177	NOD2	cis	0	0	Blood	1.22E-49
rs6500331	16	50808726	LRG_177	NOD2	cis	0	0	Blood	2.66E-19
rs7186262	16	50686959	LRG_177	NOD2	cis	0	0	Blood	1.42E-15
rs7194886	16	50725193	LRG_177	NOD2	cis	0	0	Blood	8.65E-30
rs7199150	16	50676514	LRG_177	NOD2	cis	0	0	Blood	1.48E-14
rs7342715	16	50787483	LRG_177	NOD2	cis	0	0	Blood	6.85E-20
rs745230	16	50670182	LRG_177	NOD2	cis	0	0	Blood	4.06E-14
rs748855	16	50751398	LRG_177	NOD2	cis	0	0	Blood	1.37E-21
rs749985	16	50673651	LRG_177	NOD2	cis	0	0	Blood	2.52E-14
rs751271	16	50751175	LRG_177	NOD2	cis	0	0	Blood	1.15E-08
rs8047222	16	50660962	LRG_177	NOD2	cis	0	0	Blood	6.39E-16
rs8057341	16	50737980	LRG_177	NOD2	cis	0	0	Blood	1.79E-07
rs9635531	16	50841795	LRG_177	NOD2	cis	0	0	Blood	2.87E-19
rs9938976	16	50817219	LRG_177	NOD2	cis	0	0	Blood	2.03E-24

rs9673419	16	50661273		LRG_177	NOD2	cis	0	3.10E-19	Blood	8.10E-17
rs1990623	16	50565970		LRG_177	NOD2	cis	0	2.45E-18	Blood	5.97E-11
rs2111234	16	50734033	ENSG000001	LRG_177	NOD2	Cis	0.1	1.26E-15	Blood	3.86E-08
rs8057341	16	50737980	ENSG000001	LRG_177	NOD2	Cis	0.1	3.23E-15	Blood	1.79E-07
rs1077861	16	50759547	ENSG000001	LRG_177	NOD2	Cis	0.1	9.51E-15	Blood	5.32E-11
rs751271	16	50751175	ENSG000001	LRG_177	NOD2	Cis	0.1	1.07E-13	Blood	1.15E-08
rs5743266	16	50731096	ENSG000001	LRG_177	NOD2	Cis	0.1	5.38E-06	Blood	1.22E-49
rs17221417	16	50739582	ENSG000001	LRG_177	NOD2	Cis	0.1	9.19E-06	Blood	1.45E-51
rs2297441	20	62327582		ENSG000002	RTEL1	cis	0.01	2.06E-05	Blood	1.67E-20
rs2257885	20	62334220		ENSG000002	RTEL1	cis	0.01	2.13E-05	Blood	2.62E-19
rs2427533	20	62365866		ENSG000002	RTEL1	cis	0.01	3.07E-05	Blood	1.61E-17
rs2427530	20	62361737		ENSG000002	RTEL1	cis	0.01	3.10E-05	Blood	1.07E-17
rs2738758	20	62349625		ENSG000002	RTEL1	cis	0.02	4.77E-05	Blood	2.72E-18
rs2777938	20	62306208		ENSG000002	RTEL1	cis	0.03	8.26E-05	Blood	1.07E-12
rs3016173	11	60790839		ENSG000001	SLC15A3	cis	0	2.23E-08	Blood	4.72E-07
rs175102	11	60810757		ENSG000001	SLC15A3	cis	0	2.91E-08	Blood	6.55E-07
rs11230563	11	60776209		ENSG000001	SLC15A3	cis	0	4.78E-07	Blood	9.03E-13
rs175112	11	60825022		ENSG000001	SLC15A3	cis	0	7.30E-06	Blood	1.15E-10
rs4780355	16	11347858		ENSG000001	SOCS1	cis	0	2.95E-11	Blood	1.20E-13
rs4451969	16	11383519		ENSG000001	SOCS1	cis	0	6.76E-11	Blood	2.49E-12
rs243325	16	11354497		ENSG000001	SOCS1	cis	0	1.63E-10	Blood	8.00E-14
rs243323	16	11361202		ENSG000001	SOCS1	cis	0	4.10E-10	Blood	6.12E-15
rs7193871	16	11455606		ENSG000001	SOCS1	cis	0	2.49E-09	Blood	1.33E-10
rs1646025	16	11379938		ENSG000001	SOCS1	cis	0.02	3.60E-05	Blood	5.22E-12
rs423674	16	11373405		ENSG000001	SOCS1	cis	0.02	5.65E-05	Blood	4.13E-12
rs529866	16	11373320		ENSG000001	SOCS1	cis	0.03	5.98E-05	Blood	1.49E-12
rs730086	17	40271757		LRG_112	STAT3	cis	0	1.00E-20	Blood	4.61E-10
rs957970	17	40519890		LRG_112	STAT3	cis	0	1.00E-20	Blood	2.01E-20
rs1026916	17	40529835		LRG_112	STAT3	cis	0	2.00E-20	Blood	1.48E-20
rs12949918	17	40526273		LRG_112	STAT3	cis	0	2.00E-20	Blood	2.27E-21
rs3816769	17	40498273		LRG_112	STAT3	cis	0	2.00E-20	Blood	1.55E-20
rs7211777	17	40534075		LRG_112	STAT3	cis	0	2.00E-20	Blood	2.52E-20

rs744166	17	40514201	LRG_112	STAT3	cis	0	2.00E-20	Blood	6.15E-22
rs1026916	17	40529835	LRG_112	STAT3	cis	0	8.00E-20	Blood	1.48E-20
rs7211777	17	40534075	LRG_112	STAT3	cis	0	1.10E-19	Blood	2.52E-20
rs957970	17	40519890	LRG_112	STAT3	cis	0	1.30E-19	Blood	2.01E-20
rs3816769	17	40498273	LRG_112	STAT3	cis	0	2.00E-19	Blood	1.55E-20
rs744166	17	40514201	LRG_112	STAT3	cis	0	4.10E-19	Blood	6.15E-22
rs12949918	17	40526273	LRG_112	STAT3	cis	0	7.80E-19	Blood	2.27E-21
rs730086	17	40271757	LRG_112	STAT3	cis	0	7.01E-18	Blood	4.61E-10
rs730086	17	40271757	LRG_112	STAT3	cis	0	1.08E-17	Blood	4.61E-10
rs744166	17	40514201	LRG_112	STAT3	cis	0	9.13E-17	Blood	6.15E-22
rs12949918	17	40526273	LRG_112	STAT3	cis	0	1.38E-16	Blood	2.27E-21
rs7211777	17	40534075	LRG_112	STAT3	cis	0	1.50E-16	Blood	2.52E-20
rs1026916	17	40529835	LRG_112	STAT3	cis	0	1.68E-16	Blood	1.48E-20
rs957970	17	40519890	LRG_112	STAT3	cis	0	1.88E-16	Blood	2.01E-20
rs3816769	17	40498273	LRG_112	STAT3	cis	0	2.44E-16	Blood	1.55E-20
rs4796793	17	40542210	LRG_112	STAT3	cis	0	8.40E-16	Blood	5.89E-19
rs9912773	17	40510534	LRG_112	STAT3	cis	0	1.69E-15	Blood	1.72E-18
rs3785898	17	40515120	LRG_112	STAT3	cis	0	3.65E-15	Blood	1.72E-20
rs6503695	17	40499533	LRG_112	STAT3	cis	0	3.73E-15	Blood	1.41E-20
rs8069645	17	40494902	LRG_112	STAT3	cis	0	4.68E-15	Blood	2.39E-20
rs8078731	17	40480381	LRG_112	STAT3	cis	0	7.23E-13	Blood	1.97E-11
rs9912773	17	40510534	LRG_112	STAT3	cis	0	8.88E-13	Blood	1.72E-18
rs4796793	17	40542210	LRG_112	STAT3	cis	0	1.04E-12	Blood	5.89E-19
rs12601982	17	40461674	LRG_112	STAT3	cis	0	1.11E-12	Blood	8.19E-11
rs8074524	17	40469598	LRG_112	STAT3	cis	0	1.75E-12	Blood	2.18E-12
rs2293155	17	40460989	LRG_112	STAT3	cis	0	1.84E-12	Blood	9.28E-11
rs9906989	17	40455846	LRG_112	STAT3	cis	0	2.14E-12	Blood	9.07E-11
rs1053005	17	40465910	LRG_112	STAT3	cis	0	2.34E-12	Blood	4.85E-12
rs8072215	17	40271970	LRG_112	STAT3	cis	0	2.57E-12	Blood	2.84E-07
rs3809758	17	40471980	LRG_112	STAT3	cis	0	3.04E-12	Blood	2.26E-12
rs739636	17	40281063	LRG_112	STAT3	cis	0	5.01E-12	Blood	3.10E-07
rs2293154	17	40461003	LRG_112	STAT3	cis	0	7.82E-12	Blood	9.21E-11

rs4796793	17	40542210	LRG_112	STAT3	cis		0	2.25E-11	Blood	5.89E-19
rs9912773	17	40510534	LRG_112	STAT3	cis		0	3.11E-11	Blood	1.72E-18
rs3785898	17	40515120	LRG_112	STAT3	cis		0	5.59E-11	Blood	1.72E-20
rs2293158	17	40447558	LRG_112	STAT3	cis		0	6.05E-11	Blood	4.06E-10
rs8072215	17	40271970	LRG_112	STAT3	cis		0	7.76E-11	Blood	2.84E-07
rs7217728	17	40447401	LRG_112	STAT3	cis		0	8.00E-11	Blood	4.43E-10
rs16967637	17	40446422	LRG_112	STAT3	cis		0	8.35E-11	Blood	3.43E-10
rs3785898	17	40515120	LRG_112	STAT3	cis		0	8.45E-11	Blood	1.72E-20
rs8069645	17	40494902	LRG_112	STAT3	cis		0	9.81E-11	Blood	2.39E-20
rs4029774	17	40428961	LRG_112	STAT3	cis		0	1.32E-10	Blood	1.71E-09
rs8069645	17	40494902	LRG_112	STAT3	cis		0	1.32E-10	Blood	2.39E-20
rs7209222	17	40426489	LRG_112	STAT3	cis		0	1.57E-10	Blood	8.85E-10
rs16967611	17	40401567	LRG_112	STAT3	cis		0	1.59E-10	Blood	2.53E-09
rs9906933	17	40410045	LRG_112	STAT3	cis		0	1.59E-10	Blood	1.85E-09
rs16967620	17	40422341	LRG_112	STAT3	cis		0	1.70E-10	Blood	1.69E-09
rs6503692	17	40421513	LRG_112	STAT3	cis		0	1.70E-10	Blood	3.03E-10
rs7218653	17	40425320	LRG_112	STAT3	cis		0	1.79E-10	Blood	8.14E-10
rs8064638	17	40424255	LRG_112	STAT3	cis		0	1.83E-10	Blood	1.31E-09
rs8082391	17	40398973	LRG_112	STAT3	cis		0	1.86E-10	Blood	1.91E-09
rs739636	17	40281063	LRG_112	STAT3	cis		0	1.92E-10	Blood	3.10E-07
rs6503695	17	40499533	LRG_112	STAT3	cis		0	2.07E-10	Blood	1.41E-20
rs963987	17	40561679	LRG_112	STAT3	cis		0	2.07E-10	Blood	5.03E-12
rs2883456	17	40552794	LRG_112	STAT3	cis		0	2.55E-10	Blood	6.69E-12
rs744166	17	40514201	LRG_112	STAT3	Cis	NA		2.12E-09	Whole blood	6.15E-22
rs6503695	17	40499533	LRG_112	STAT3	cis		0	2.57E-09	Blood	1.41E-20
rs2883456	17	40552794	LRG_112	STAT3	cis		0	4.92E-09	Blood	6.69E-12
rs963987	17	40561679	LRG_112	STAT3	cis		0	5.15E-09	Blood	5.03E-12
rs12601982	17	40461674	LRG_112	STAT3	cis		0	6.26E-08	Blood	8.19E-11
rs11079045	17	40587669	LRG_112	STAT3	cis		0	7.86E-08	Blood	4.55E-10
rs8078731	17	40480381	LRG_112	STAT3	cis		0	9.16E-08	Blood	1.97E-11
rs2293155	17	40460989	LRG_112	STAT3	cis		0	1.01E-07	Blood	9.28E-11
rs8078731	17	40480381	LRG_112	STAT3	cis		0	1.17E-07	Blood	1.97E-11

rs11079045	17	40587669		LRG_112	STAT3	cis		0	1.27E-07	Blood	4.55E-10
rs9906989	17	40455846		LRG_112	STAT3	cis		0	1.49E-07	Blood	9.07E-11
rs8072215	17	40271970		LRG_112	STAT3	cis		0	1.67E-07	Blood	2.84E-07
rs12601982	17	40461674		LRG_112	STAT3	cis		0	2.60E-07	Blood	8.19E-11
rs739636	17	40281063		LRG_112	STAT3	cis		0	3.15E-07	Blood	3.10E-07
rs2293155	17	40460989		LRG_112	STAT3	cis		0	3.65E-07	Blood	9.28E-11
rs2293154	17	40461003		LRG_112	STAT3	cis		0	3.90E-07	Blood	9.21E-11
rs744166	17	40514201		LRG_112	STAT3	Cis	NA		4.53E-07	Whole blood	6.15E-22
rs9906989	17	40455846		LRG_112	STAT3	cis		0	4.94E-07	Blood	9.07E-11
rs2293154	17	40461003		LRG_112	STAT3	cis		0	6.94E-07	Blood	9.21E-11
rs8074524	17	40469598		LRG_112	STAT3	cis		0	7.72E-07	Blood	2.18E-12
rs3809758	17	40471980		LRG_112	STAT3	cis		0	7.87E-07	Blood	2.26E-12
rs1053005	17	40465910		LRG_112	STAT3	cis		0	9.04E-07	Blood	4.85E-12
rs744166	17	40514201	---	LRG_112	STAT3	Cis		0.1	1.00E-06	Blood	6.15E-22
rs963987	17	40561679		LRG_112	STAT3	cis		0	1.37E-06	Blood	5.03E-12
rs2883456	17	40552794		LRG_112	STAT3	cis		0	1.59E-06	Blood	6.69E-12
rs8074524	17	40469598		LRG_112	STAT3	cis		0	3.44E-06	Blood	2.18E-12
rs1053005	17	40465910		LRG_112	STAT3	cis		0	4.41E-06	Blood	4.85E-12
rs3809758	17	40471980		LRG_112	STAT3	cis		0	4.78E-06	Blood	2.26E-12
rs1905339	17	40582296		LRG_112	STAT3	cis		0	8.40E-06	Blood	4.20E-07
rs11079045	17	40587669		LRG_112	STAT3	cis		0.01	1.60E-05	Blood	4.55E-10
rs2293158	17	40447558		LRG_112	STAT3	cis		0.02	3.52E-05	Blood	4.06E-10
rs16967637	17	40446422		LRG_112	STAT3	cis		0.02	4.48E-05	Blood	3.43E-10
rs7217728	17	40447401		LRG_112	STAT3	cis		0.02	4.58E-05	Blood	4.43E-10
rs4029774	17	40428961		LRG_112	STAT3	cis		0.03	6.74E-05	Blood	1.71E-09
rs7209222	17	40426489		LRG_112	STAT3	cis		0.03	7.40E-05	Blood	8.85E-10
rs16967611	17	40401567		LRG_112	STAT3	cis		0.03	7.65E-05	Blood	2.53E-09
rs8082391	17	40398973		LRG_112	STAT3	cis		0.03	7.65E-05	Blood	1.91E-09
rs16967620	17	40422341		LRG_112	STAT3	cis		0.03	7.91E-05	Blood	1.69E-09
rs6503692	17	40421513		LRG_112	STAT3	cis		0.03	7.91E-05	Blood	3.03E-10
rs9906933	17	40410045		LRG_112	STAT3	cis		0.03	8.01E-05	Blood	1.85E-09
rs7218653	17	40425320		LRG_112	STAT3	cis		0.03	8.28E-05	Blood	8.14E-10

rs8064638	17	40424255	LRG_112	STAT3	cis	0.03	8.28E-05	Blood	1.31E-09
rs2293154	17	40461003	ENSG00000	STAT5A	cis	0	5.62E-07	Blood	9.21E-11
rs12601982	17	40461674	ENSG00000	STAT5A	cis	0	6.57E-07	Blood	8.19E-11
rs2293155	17	40460989	ENSG00000	STAT5A	cis	0	7.65E-07	Blood	9.28E-11
rs9906989	17	40455846	ENSG00000	STAT5A	cis	0	8.49E-07	Blood	9.07E-11
rs8078731	17	40480381	ENSG00000	STAT5A	cis	0	8.51E-07	Blood	1.97E-11
rs8074524	17	40469598	ENSG00000	STAT5A	cis	0	9.86E-07	Blood	2.18E-12
rs1053005	17	40465910	ENSG00000	STAT5A	cis	0	1.17E-06	Blood	4.85E-12
rs3809758	17	40471980	ENSG00000	STAT5A	cis	0	1.30E-06	Blood	2.26E-12
rs6503695	17	40499533	ENSG00000	STAT5A	cis	0.01	1.69E-05	Blood	1.41E-20
rs8064638	17	40424255	ENSG00000	STAT5A	cis	0.01	1.97E-05	Blood	1.31E-09
rs9906933	17	40410045	ENSG00000	STAT5A	cis	0.01	1.98E-05	Blood	1.85E-09
rs16967611	17	40401567	ENSG00000	STAT5A	cis	0.01	2.08E-05	Blood	2.53E-09
rs4029774	17	40428961	ENSG00000	STAT5A	cis	0.01	2.11E-05	Blood	1.71E-09
rs7209222	17	40426489	ENSG00000	STAT5A	cis	0.01	2.11E-05	Blood	8.85E-10
rs16967620	17	40422341	ENSG00000	STAT5A	cis	0.01	2.23E-05	Blood	1.69E-09
rs6503692	17	40421513	ENSG00000	STAT5A	cis	0.01	2.23E-05	Blood	3.03E-10
rs16967637	17	40446422	ENSG00000	STAT5A	cis	0.01	2.24E-05	Blood	3.43E-10
rs7218653	17	40425320	ENSG00000	STAT5A	cis	0.01	2.27E-05	Blood	8.14E-10
rs2293158	17	40447558	ENSG00000	STAT5A	cis	0.01	2.28E-05	Blood	4.06E-10
rs7217728	17	40447401	ENSG00000	STAT5A	cis	0.01	2.28E-05	Blood	4.43E-10
rs8082391	17	40398973	ENSG00000	STAT5A	cis	0.01	2.38E-05	Blood	1.91E-09
rs8069645	17	40494902	ENSG00000	STAT5A	cis	0.02	3.63E-05	Blood	2.39E-20
rs3785898	17	40515120	ENSG00000	STAT5A	cis	0.02	3.78E-05	Blood	1.72E-20
rs4796793	17	40542210	ENSG00000	STAT5A	cis	0.02	4.21E-05	Blood	5.89E-19
rs9912773	17	40510534	ENSG00000	STAT5A	cis	0.02	4.65E-05	Blood	1.72E-18
rs10114470	9	117547772	ENSG00000	TNFSF8	cis	0	0	Blood	1.02E-30
rs1322055	9	117669585	ENSG00000	TNFSF8	cis	0	0	Blood	2.87E-09
rs3810936	9	117552885	ENSG00000	TNFSF8	cis	0	0	Blood	3.64E-31
rs4246905	9	117553249	ENSG00000	TNFSF8	cis	0	0	Blood	2.80E-32
rs4263839	9	117566440	ENSG00000	TNFSF8	cis	0	0	Blood	3.53E-31
rs4574921	9	117538334	ENSG00000	TNFSF8	cis	0	0	Blood	5.05E-29

rs6478108	9	117558703	ENSG00000117TNFSF8	cis	0	0	Blood	4.05E-31
rs7040029	9	117619214	ENSG00000117TNFSF8	cis	0	0	Blood	5.48E-23
rs7848647	9	117569046	ENSG00000117TNFSF8	cis	0	0	Blood	5.02E-31
rs7866342	9	117627569	ENSG00000117TNFSF8	cis	0	0	Blood	3.16E-21
rs911605	9	117654990	ENSG00000117TNFSF8	cis	0	0	Blood	1.16E-19
rs7048659	9	117533289	ENSG00000117TNFSF8	cis	0	2.76E-16	Blood	1.10E-07
rs10114224	9	117613032	ENSG00000117TNFSF8	cis	0	1.11E-15	Blood	6.63E-09
rs10982427	9	117613696	ENSG00000117TNFSF8	cis	0	1.11E-15	Blood	1.62E-08
rs10982441	9	117647599	ENSG00000117TNFSF8	cis	0	1.26E-15	Blood	8.69E-07
rs7865494	9	117576479	ENSG00000117TNFSF8	cis	0	5.91E-15	Blood	3.70E-11
rs1419134	9	117587022	ENSG00000117TNFSF8	cis	0	1.42E-14	Blood	4.13E-11
rs2145929	9	117581940	ENSG00000117TNFSF8	cis	0	3.14E-14	Blood	1.36E-11
rs7868351	9	117584082	ENSG00000117TNFSF8	cis	0	8.95E-14	Blood	1.65E-11
rs10982412	9	117570856	ENSG00000117TNFSF8	cis	0	1.42E-12	Blood	2.52E-10
rs17292046	9	117587092	ENSG00000117TNFSF8	cis	0	2.39E-11	Blood	4.68E-10
rs10982396	9	117518929	ENSG00000117TNFSF8	cis	0	3.64E-11	Blood	6.90E-10
rs10759736	9	117523192	ENSG00000117TNFSF8	cis	0	3.70E-11	Blood	4.59E-10
rs7862325	9	117567137	ENSG00000117TNFSF8	cis	0	8.71E-11	Blood	2.90E-07
rs13300483	9	117643362	ENSG00000117TNFSF8	cis	0	5.87E-10	Blood	4.48E-14
rs7860414	9	117541450	ENSG00000117TNFSF8	cis	0	4.13E-09	Blood	8.50E-11
rs1407308	9	117570223	ENSG00000117TNFSF8	cis	0	8.43E-09	Blood	1.50E-07
rs7866570	9	117577189	ENSG00000117TNFSF8	cis	0	9.24E-09	Blood	1.26E-07
rs10982433	9	117620404	ENSG00000117TNFSF8	cis	0	1.32E-08	Blood	1.33E-11
rs16931895	9	117609919	ENSG00000117TNFSF8	cis	0	2.58E-08	Blood	1.80E-13
rs10982417	9	117589613	ENSG00000117TNFSF8	cis	0	2.78E-08	Blood	4.03E-14
rs2093403	9	117611913	ENSG00000117TNFSF8	cis	0	3.12E-08	Blood	2.03E-12
rs4262377	9	117589574	ENSG00000117TNFSF8	cis	0	3.66E-08	Blood	7.08E-14

Table S9: TRIM22 Sub network Annotation

Gene	Alias	Category- Excerpt of reference	PMID
ADAR	ADAR1	Inhibits HIV in macs, interferon induction.	PMID: 25456137
FTSJD2		Methyltransferase responsible for cap1 formation in human cells, first nucleotide of a capped nucleotide in RNA.	PMID: 20713356
CIITA		MHCII transcription activation	PMID: 17043423
RFX5		NLRC5 cooperates with the RFX transcription factor complex to induce MHC class I gene expression.	PMID: 22490869 , PMID: 1210125
LILRB4	ILT3	The upregulated expression of BCL6, SOCS1 and DUSP10 is integral to the signature of ILT3-Fc-induced CD8(+) T cells. These genes are known inhibitors of cytokine production and TCR signaling and is a marker for CD8 T suppressor cells.	PMID: 23018130
CLEC1A		Natural killer c type lectin receptor	
FPR3		H. pylori-derived peptide Hp(2-20) stimulates eosinophil migration through the engagement of FPR2 and FPR3, and also induces production of VEGF-A and TGF-beta, two key mediators of tissue remodelling.	PMID: 24067461
CXCR6		The chemokine receptor CXCR6 controls the functional topography of interleukin-22 producing intestinal innate lymphoid cells.	PMID: 25456160
NAPSB		Napsin B aspartic peptidase	
GNGT2		Phototransduction in retina	
GNAI2		Gnai2 expression affects marginal zone B-cell development, splenic architecture, lymphoid follicle size, and germinal center morphology. Gnai2 expression is also needed for the proper alignment of MOMA-1(+) macrophages and MAdCAM-1(+) endothelial cells along marginal zone sinuses in the spleen.	PMID: 20508603
SLC2A6	GLUT6/9	Cell metabolism	
CSF2RA		Auto antibodies correlating with aggressive disease.	PMID: 24503766
ICOS		ICOS Coreceptor Signaling Inactivates the Transcription Factor FOXO1 to Promote Tfh Cell Differentiation. ICOS is required for the generation of both central and effector CD4+ memory T-cell populations following acute bacterial infection.	PMID: 25754933
ST3GAL5	GM3	and integrin-mediated cell adhesion. The protein encoded by this gene is a type II membrane protein which catalyzes the formation of GM3 using lactosylceramide as the substrate.	PMID: 26362868
SLC39A4		A mouse model of acrodermatitis enteropathica: loss of intestine zinc transporter ZIP4 (Slc39a4) disrupts the stem cell niche and intestine integrity.	PMID: 22737083
FAM65B		Fam65b negatively regulates chemokine-induced responses, such as adhesion, morphological polarization, and migration. Fam65b is a new transcriptional target of FOXO1 that regulates RhoA signaling for T lymphocyte migration.	PMID: 25588844
LAP3		Autophagy in yeast	
CXCL9		Anti microbial response: CXCR3 Chemokine Receptor Enables Local CD8+ T Cell Migration for the Destruction of Virus-Infected Cells in Skin.	PMID: 25643352, PMID: 2576961
CD40LG		Involved in activation and antigen presentation. Related to hyper IgM and is under selective pressure.	PMID: 26644385
NFAM1		NFAM1 modulates B cell signaling through its ITAM, calcineurin/NFAT-activating and immunoreceptor tyrosine-based activation motif (ITAM)-containing protein (CNAIP) Y+TNF induced and activated TNF.CNAIP was preferentially expressed in neutrophils, monocytes, mast cells, and other immune-related cells. Activates TNFa and IL13 promoters.	PMID: 15143214, PMID: 1261591
ELK2AP	ELK	Elk-1 is a transcription factor whose activation by several mitogen-activated protein kinases (MAPKs) mediates the immediate early responses of the c-fos promoter to growth factors and other stimuli. In heavy chain IGH gene, ELK2 is a pseudo gene.	
MMP25	MT6-MMP	MT6-MMP regulates neutrophil and monocyte chemotaxis and by generating "eat-me" signals upon vimentin cleavage potentially increases phagocytic removal of neutrophils to resolve inflammation.	PMID: 22367194
LRRC33		Identification and characterization of a unique leucine-rich repeat protein (LRRC33) that inhibits Toll-like receptor-mediated NF-κB activation.	PMID: 23545260
GM2A	GM2-AP, SAP-3	An activator protein which stimulates the enzymatic hydrolysis of N-acetylneuraminic acid, but not N-acetylgalactosamine, from GM2. Suggested roles of Saps is their deregulating effect on various proteolytic cascades that constitute the major homeostatic systems in human hosts, including blood coagulation, fibrinolysis, and kallikrein-kinin systems, and SAP3 generated proinflammatory bradykinin-related peptides (kinins).	PMID: 8631864 , PMID: 25777036
CECR1	ADA2	Human adenosine deaminase 2 induces differentiation of monocytes into macrophages and stimulates proliferation of T helper cells and macrophages. Identified biallelic CECR1 mutations in two patients consistent with ADA2 deficiency. Both patients demonstrated an upregulation of interferon stimulated gene transcripts in peripheral blood.	PMID: 20453107, PMID: 2527881
GNB4	CMTD1F	GNB isoforms are required for LFA-1 activation and chemokine induced downstream signal Rac-1, PlcB2, PlcB3.	PMID: 26468229
CD86		Upregulation on IECs is correlated with disease activity.	PMID: 25574091
SNX10		Endosomal sorting nexin	PMID: 26141367
GZMB		Granzyme B-activated p53 interacts with Bcl-2 to promote cytotoxic lymphocyte-mediated apoptosis.	PMID: 26156785
MMP19		MMP19 and MMP23B belong to the Matrix metalloproteases (MMPs) family, which are zinc-binding endopeptidases that are capable of degrading various components of the extracellular matrix.	PMID: 18523579
PLA2G4F		Pla2g4f, a phospholipase and Duox2 are colitis gene candidates- GPX metabolizes PLA2G4F and DUOX2 products.	PMID: 20872835
KDM2B		The H3K36 demethylase Jhdm1b/Kdm2b regulates cell proliferation and senescence through p15(Ink4b).	PMID: 26237645
GPSM3		G Protein signaling modulator-3 inhibits the inflammasome activity of NLRP3, and is involved in monocyte chemotaxis.	
PDCD1LG2	PDL2	Regulation of T cell activation and tolerance by PDL2, which is positively regulated by IRF1.	PMID:25053811
C1S		Complement	
DRAM1		Regulates apoptosis, promotes targeting of mycobacteria to autophagy, the induction of the DNA damage-regulated autophagy modulator DRAM1 via the toll-like receptor (TLR)-MYD88-NFKB innate immunity signaling pathway/ p53 target gene that regulates autophagy and apoptosis.	PMID: 25484076
SDC3	SDCN, SYND3	Syndecan-3 is a dendritic cell-specific attachment receptor for HIV-1, heparan sulfate (HS) proteoglycan .	PMID: 18040049
LILRB2		LILRB2 interaction with HLA class I correlates with control of HIV-1 infection.	PMID: 24603468
CCDC71L	C7orf74	Gene related to athlerosclerosis.	
PLA2G7		Arachodinic acid program, upregulated upon neutrophil stimulation.	PMID: 26348085
SENP7		scenescence.	PMID: 26527005
PLXNC1		The plexin receptor is involved in acute inflammation and leukocyte migration. Plexin C1 (VESPR/CD232) is identified as being involved in sCD100-mediated (expressed in immature DCs) effects on human monocytes. Down-regulation of plexin C1 expression during the in vitro differentiation process of monocytes to immature DCs, while concomitantly the surface expression of plexin B1 was induced.	PMID: 15746246, PMID: 1574624
TMEM71		ING2, in the P53 pathway, can be sumoylated by small ubiquitin-like modifier 1 (SUMO1) on lysine 195 both in vitro and in vivo.ING2 sumoylation enhances its association with Sin3a. TMEM71 (transmembrane protein 71) expression is regulated by ING2 sumoylation.	PMID: 20676127
ASB2		We show that not only NOTCH but also ASB2 and SKP2 can promote the ubiquitination and degradation of JAK3. Also involved in immature DC migration, ASB2α-mediated effects on cell spreading are due to loss of filamins.	PMID: 21969365
COL1A1		Noncanonical STAT3 Activation Regulates Excess TGF-β1 and Collagen I Expression in Muscle of Stricturing Crohn's Disease.	PMID: 25740948
AKAP11	AKAP220	AKAP220/IQGAP1 networks receive and integrate calcium and cAMP second messenger signals and position signaling enzymes near their intended substrates at leading edges of migrating cells.	PMID: 21890631
MX2		Interferon induced anti viral restriction factor	PMID: 24760893
SPIB		essential for the differentiation of intestinal microfold cells. Peyer's patch M cells derived from Lgr5(+) stem cells require SpiB and are induced by RankL in cultured "miniguts".	PMID: 23439650 , PMID: 2270634
CD1E		The interaction of LAPTM5 with CD1e and their colocalization in antigen processing compartments both suggest that LAPTM5 might influence the role of CD1e in the presentation of lipid antigens.	PMID: 22880058
MTX3		Metaxin deficiency alters mitochondrial membrane permeability and leads to resistance of TNF induced killing.	PMID: 21088703
UBE2E2	UBCH8	UbcH8, an ubiquitin E2 conjugating enzyme, was shown to be involved in RIG-I ISGylation. UbcH8 suppressed RIG-I ubiquitination by RNF125, and this suppression was relieved by ectopic expression of ISG15.	PMID:25960396
CXCL5		Neutrophil recruitment. De-regulation in the intestinal epithelium in perdiatric IBD reported in this pathway.	PMID: 25738378
ARID5A		AT-rich-interactive domain-containing protein 5A functions as a negative regulator of retinoic acid receptor-related orphan nuclear receptor γt-induced Th17 cell differentiation. Controls IL6 levels.	PMID: 23676272
TIMP1		MMP-3 and TIMP-1: inhibitor of MMPs activity by myofibroblast involved in ulcers in CD.	PMID: 24583398
SIGLEC9		Binding of the sialic acid-binding lectin, Siglec-9, to the membrane mucin, MUC1, induces recruitment of β-catenin and subsequent cell growth. Colonic epithelial cells express specific ligands for mucosal macrophage immunosuppressive receptors siglec-7 and -9. 9 turned out to be resident macrophages characterized by low expression of CD14/CD89 and high expression of CD68/CD163. A minor subpopulation of CD8(+) T lymphocytes also expressed siglec-7/-9. Siglec-7/-9 ligation suppressed LPS-induced cyclooxygenase-2 expression and PGE(2) production by macrophages.	PMID: 24045940 , PMID: 2246765
TIFA		Intermolecular binding between TIFA-FHA and TIFA-pT mediates tumor necrosis factor alpha stimulation and NF-κB activation. Identification of TIFA as an adapter protein that links tumor necrosis factor receptor-associated factor 6 (TRAF6) to interleukin-1 (IL-1) receptor-associated kinase-1 (IRAK-1) in IL-1 receptor signaling.	PMID: 22566686, PMID: 1256644
TNFRSF6B	DCR3	Targeted resequencing identifies defective variants of decoy receptor 3 in pediatric-onset inflammatory bowel disease, Differential expression of the TL1A/DcR3 system of TNF/TNFR-like proteins in large vs. small intestinal Crohn's disease, High intestinal and systemic levels of decoy receptor 3 (DcR3) and its ligand TL1A in active ulcerative colitis. An additive gene-gene interaction involving TLR4, PSMG1, TNFRSF6B and IRGM was identified with CD.	PMID: 23965943 , PMID: 2197857
CEBPB		Inflammatory cytokine production by human neutrophils involves C/EBP transcription factors.	PMID: 19109189
PARP9		DTX3L and ARTD9 inhibit IRF1 expression and mediate in cooperation with ARTD8 survival and proliferation of metastatic prostate cancer cells.	PMID: 23487038
CENPV		Kinetochore/ mitotic spindles	
CD40		The interaction between CD40 and its ligand, CD40L/CD154, is crucial for the efficient initiation and regulation of immune responses against viruses.	PMID: 25765994
DOK3		DOK3 is required for IFN-β production by enabling TRAF3/TBK1 complex formation and IRF3 activation. Also involved in LPS response in macrophages.	PMID: 24929003
S1PR4		S1PR4 is required for plasmacytoid dendritic cell differentiation.	PMID: 25720060
GMFG		Glia maturation factor-γ negatively modulates TLR4 signaling by facilitating TLR4 endocytic trafficking in macrophages. GMFG is a component of human T cell pseudopodia required for migration. Glia maturation factor-γ mediates neutrophil chemotaxis.	PMID: 23677465, PMID: 2251051
ACP5		A tartrate-resistant acid phosphatase. Disruption of the gene results in elevated serum interferon alpha activity, and gene expression profiling in whole blood defined a type I interferon signature.	PMID: 21217755
TNFAIP2		Inhibits NFKB and is an autoinhibitor of TNF during sepsis.	PMID: 22078882, PMID: 2634748
LYST		Lysosomal trafficking regulator. LYST controls the biogenesis of the endosomal compartment required for secretory lysosome function.	PMID: 25425525
VPS13C		Glucose insulin metabolism (potentially autophagy)	PMID: 22956255
HV1	HVCN1	Involved in eosinophil effector functions, HV1 is among genes which correlate significantly with Crohn's clinical activity. Hv1 proton channels differentially regulate the pH of neutrophil and macrophage phagosomes by sustaining the production of phagosomal ROS that inhibit the delivery of vacuolar ATPases.	PMID: 23437289, PMID: 2441579
KCNAB2		Voltage pottassium channel	
ITGB2	CD18	CD11b/CD18 (Mac-1) is a novel surface receptor for extracellular double-stranded RNA to mediate cellular inflammatory responses. DNA methylation-associated colonic mucosal immune and defense responses in treatment-naïve pediatric ulcerative colitis.	PMID: 23209319
CLEC7A		Downregulated by Th17, polymorphism in the gene for Dectin-1 (CLEC7A) is strongly linked to a severe form of ulcerative colitis.	PMID: 22674328

CXCL6		Neutrophil cytokine in response to IEC cell line cultured with TNF and IL17.	PMID: 26617980
LIMS3L		LIM and senescent cell antigen-like domains 3-like	
PLEKHO2		Identification of pleckstrin-homology-domain-containing proteins with novel phosphoinositide-binding specificities in signalling.	
FBXO6	FBS2	Fbs2 is a new member of the E3 ubiquitin ligase family that recognizes sugar chains.. Inhibits ER stress by functioning as ubiquitin ligase in ERAD system.	PMID: 12939278, PMID: 2537437
SLAMF8		Slamf8 is a negative regulator of Nox2 activity in macrophages.	PMID: 22593622
PSTPIP2		Associated with autoinflammatory disease and anti HCV replication.	PMID: 22130530, PMID: 2439580
NCF2		NADPH / NCF2/p67phox: A novel player in the anti-apoptotic functions of p53 and can be induced by TNFα.	PMID: 21900546
IL27RA		Activation of IL-27 signalling promotes development of postinfluenza pneumococcal pneumonia.In response to il10, supresses Th17 1l17 and ifng related processes, copy induces TH1, also can be anti viral.	PMID: 24408967, PMID: 2508899
ARHGAP30		ArhGAP30 promotes p53 acetylation and function in colorectal cancer.	PMID: 25156493
CSF3R		G-CSF preferentially supports the generation of gut-homing Gr-1high macrophages in M-CSF-treated bone marrow cells.	PMID: 24503766, PMID: 2498162
MNDA		The human PYHIN proteins, AIM2, IFI16, IFIX, and MNDA, are critical regulators of immune response, transcription, apoptosis, and cell cycle.	
FAH		Fumarylacetoacetate hydrolase- an enzyme that catalyzes the last step of tyrosine metabolism.	PMID: 24879068
CLEC4A	DCIR	DCIR-mediated enhancement of HIV-1 infection requires the ITIM-associated signal transduction pathway. DCIR is endocytosed into human dendritic cells and inhibits TLR8-mediated cytokine production.	PMID: 19028959
PTAFR	PAF	Associated with pneumoccocal disease, PAF signaling in peritoneal macrophages requires TLR4, MyD88, and TRIF. In peritoneal macrophages, the PTAFR agonist carbamyl PAF induces production of inflammatory markers previously demonstrated to be upregulated during bacterially induced labor, including: inducible nitric oxide synthase (Nos2), the chemokine Ccl5 (RANTES), tumor necrosis factor (Tnf), and level of their end-products (NO, CCL5, TNF) in a process dependent upon both IkappaB kinase and calcium/calmodulin-dependent protein kinase II.	PMID: 25253732, PMID: 2525373
CD300A		PPARβ/δ activation of CD300a controls intestinal immunity in M1 macs and binds phophatidyserine on dying cells.	PMID: 24958459
CDC42SE1	SPEC1	SPECs may play important roles in Cdc42-mediated F-actin accumulation at the immunological synapse.	PMID: 15840583
GBP4		GBP4 is a negative regulator of virus-triggered IFN-I production, and it is identified as a novel protein targeting IRF7 and inhibiting its function.	PMID: 23029268, PMID: 2209571
KYNU		Kynureninase involved in the L-tryptophan aerobic degradation pathway.	PMID: 26347385, PMID: 2634738
TLR8		Toll-like receptor 8 (TLR8) was required for inducing pro-IL-1β expression, whereas the NLRP3 inflammasome was required for IL-1β maturation and release.	PMID: 24939850
BID		Tumor necrosis factor alpha triggers Bid-dependent lysosomal permeabilization, followed by release of cathepsin B into the cytosol and activation of caspase 2. Caspase 2 then facilitates efficient mitochondrial cytochrome c release and apoptosis.	PMID: 16012953, PMID: 1601295
FGR		Src family kinases were required for the generation of the inflammatory environment in vivo and for the release of proinflammatory mediators from neutrophils and macrophages in vitro, likely due to their role in Fcγ receptor signal transduction, but not involved in recruitment. ROS-triggered phosphorylation of complex II by Fgr kinase regulates cellular adaptation to fuel use.	PMID: 25225462, PMID: 2485693
SLAMF7	CS1	monocytes.	PMID: 23695528
IGSF6	DORA	Downregulated by CD40L on DCs. This structure and expression protein belonging to the CD8 family suggests a function as a co-receptor, perhaps in an antigen uptake complex, or in homing or recirculation of DC.	PMID: 9809579
DYSF		Inflammasome up-regulation and activation in dysferlin-deficient skeletal muscle.	PMID: 20413686
F2R	PAR1	Protease-activated receptor-1 (PAR1) is a G protein-coupled receptor that is classically activated through cleavage of the N-terminal exodomain by the serine protease thrombin. Most recently, 2 MMPs have been discovered to have agonist activity for PAR1:MMP-1 and MMP-13	PMID: 23086754
EMR2		EMR2 receptor ligation modulates cytokine secretion profiles and cell survival of lipopolysaccharide-treated neutrophils. CD312, the human adhesion-GPCR EMR2, is differentially expressed during differentiation, maturation, and activation of myeloid cells.	PMID: 22035891, PMID: 1717427
LILRA5		LILRA5 is expressed by synovial tissue macrophages in rheumatoid arthritis, selectively induces pro-inflammatory cytokines and IL-10 and is regulated by TNF-alpha, IL-10 and IFN-gamma.	PMID:19009525
EMILIN2		Regulation of the extrinsic apoptotic pathway by the extracellular matrix glycoprotein EMILIN2.	PMID: 17698584
TBXAS1		Thromboxane A synthase (TBXAS1) converts prostaglandin H to thromboxane A.	
IRF1		A distal locus element mediates IFN-γ priming of lipopolysaccharide-stimulated TNF gene expression. Data suggests that during intestinal inflammation, the TNF-α-mediated activation of IRF1 is related to the subsequent suppression of OPN expression, further reducing p-AKT, p-P38, and p-ERK activities and resulting in aggravation of the injury to intestinal epithelial cells.	PMID: 25482561, PMID: 2520810
ZYX	ESP-2, HED-2	ZYX-1 protein is expressed in the striated body-wall muscles and is involved in dystrophin-dependent muscle.	
GBP1P1		Gamma interferon-induced guanylate binding protein 1 is a novel actin cytoskeleton remodeling factor.	PMID: 24190970
APOL4		Lipid exchange and transport	
FCGR3A	CD16	Associated with susceptibility to autoimmunity. Influences response to Infliximab through ADCC.	PMID: 26407570, PMID: 2335893
UBE2D1	UBCH5	UbcH5 is an E2 ubiquitin-conjugating enzyme catalyzing ubiquitination during TNF-α-triggered NF-κB activation. Inhibition leads to p53 apoptosis.	PMID: 25200604
GPNMB		Lysosomal stress in obese adipose tissue macrophages contributes to MITF-dependent Gpnmb induction.	PMID: 24789918
MRAS	RRAS3	Ras oncogene, MRAS, through its ability to recruit a complex with paradoxical components, coordinates ERK pathway. Involved in intestinal fibrosis in CD rats.	PMID: 23970928, PMID: 2386348
DNASE2		Seven nonsynonymous SNPs in the gene encoding human deoxyribonuclease II may serve as a functional SNP potentially implicated in autoimmune dysfunction.	PMID: 24242851
MSANTD3		Anti viral response, DNA binding.	PMID: 25547032
LIMS3	PINCH3	Pinch-3 protein is an important constituent of cell membranes, which directly affects the cell morphology and mechanical properties.	PMID: 23865313
IL2RA		Il2 receptor chain expressed on FoxP3 regulatory T cells.	PMID: 24483245
PLEK	p47	p47 negatively regulates IKK activation by inducing the lysosomal degradation of polyubiquitinated NEMO.	PMID: 22990857
STAT1		Mendelian myco bacteria response, type I and type II interferon signalling.	
PML		Induction of IFNB	PMID: 25733689
TGFB	TGFB1	Controls proliferation and cellular differentiation. Involved in wound healing and mucosal immunity.	PMID: 26559094
SOCS1		Expression of suppressor of cytokine signaling 1 (SOCS1) impairs viral clearance and exacerbates lung injury during influenza infection. Has been reported to play an important role in Treg cell integrity and function by protecting the cells from excessive inflammatory cytokines. Co-immunoprecipitation studies revealed that SOCS1 physically interacted with RhTRIM5α.	PMID: 25500584, PMID: 2513319
DNAJC5B	CSP-beta	Cysteine string proteins (CSPs) are associated with regulated secretory organelles.	
CTLA4		P695. A mutation in CTLA4 associated with early-onset Crohn's disease and autoimmunity.	PMID: 25718204
SLC43A3		A candidate gene linking systemic inflammation to atherosclerosis; results of a human in vivo LPS infusion study.	PMID: 21827714
CHST2		CHST1 and CHST2 contribute to the generation of optimal L-selectin ligands in vascular endothelial cells at sites of inflammation.	PMID: 11310842
MAP3K8		Pharmacological inhibition of TPL2/MAP3K8 blocks human cytotoxic T lymphocyte effector functions.TPL2 mediates autoimmune inflammation through activation of the TAK1 axis of IL-17 signaling.	PMID: 24642963, PMID: 2498004
BATF2		IFN induced, interact with IRF, DCs	PMID: 23787991
CXCL10		NOD2 synergized with IFN-γ to induce CXCL9 and CXCL10 secretion in dendritic cells, macrophages, and intestinal stromal cells in vitro.	PMID: 24591373
APOL1		APOL1 expression is induced by proinflammatory cytokines gamma interferon (IFN-γ) and tumor necrosis factor alpha (TNF-α).	PMID: 24173214
APOL2		A novel anti-apoptotic role for apolipoprotein L2 in IFN-γ-induced cytotoxicity in human bronchial epithelial cells.	PMID: 20665705
PDE4B		Inhibition of PDE4B suppresses inflammation by increasing expression of the deubiquitinase CYLD.	PMID: 23575688, PMID: 2574878
IL15RA		Type I interferon related TB response. IL-15 modulates the balance between Bcl-2 and Bim via a Jak3/1-PI3K-Akt-ERK pathway to promote CD8αα+ intestinal intraepithelial lymphocyte survival.	PMID: 23754237
CD274		Biochemical signaling of PD-1 on T cells and its functional implications.	PMID: 25098287
SLC2A3	GLUT3	Hypoxia/IL-10 showed the enhanced induction of a set of genes including PLOD2 and SLC2A3. In cancer, mTORC1 enhances Glut3 expression through the activation of the IKK/NFκB pathway.	PMID: 25450522
NNMT		Related to pathogenesis of metabolic disease.	
IL10RA		Clinical features of interleukin 10 receptor gene mutations in children with very early-onset inflammatory bowel disease.	PMID: 25373860
IFI30		γ-Interferon-inducible lysosomal thiol reductase (GILT) maintains phagosomal proteolysis in alternatively activated macrophages.GILT expression in B cells diminishes cathepsin S steady-state protein expression and activity.	PMID: 25253686
ITPRIP	DANGER	DANGER, a novel regulatory protein of inositol 1,4,5-trisphosphate-receptor activity. Individual subtypes of enteroendocrine cells in the mouse small intestine exhibit unique patterns of inositol 1,4,5-trisphosphate receptor expression.	PMID: 14688217
SCIMP		SCIMP, a transmembrane adaptor protein involved in major histocompatibility complex class II signaling.	PMID: 21930792
GFI1		The transcription factor GFI1 negatively regulates NLRP3 inflammasome activation in macrophages. There are many other transcription factors, such as RUNX family proteins, IRF4, Dec2, Gfi1, Hlx, and JunB that can impair TH1/TH2 cells differentiation.	PMID: 25447538, PMID: 2526120
DTX1		E3 Ubiquitin ligase, Deltex1 antagonizes HIF-1α and sustains the stability of regulatory T cells in vivo, Deltex1 is a target of the transcription factor NFAT that promotes T cell anergy.	PMID: 25695215, PMID: 1959227
CP	CP-2	Ceruloplasmin (ferroxidase) / iron.	
CFH		Complement Factor H. Intestinal glycoprotein activates the alternative complement pathway by reacting with factor H.	PMID: 6213029
GBP5		GBP5 promotes NLRP3 inflammasome assembly and immunity in mammals.	PMID: 22461501
BASP1		Repression of transcription by WT1-BASP1 requires the myristoylation of BASP1 and the PIP2-dependent recruitment of histone deacetylase./ apoptosis.	PMID: 22939983
TRIM22			
TRIM5		TRIM proteins regulate autophagy: TRIM5 is a selective autophagy receptor mediating HIV-1 restriction and is a ubiquitin ligase that stimulates type I interferon & NFKB pathways with TRAF6.	PMID: 25587751, PMID: 2650395
TRIM38		TRIM38 inhibits TNFα- and IL-1β-triggered NF-κB activation by mediating lysosome-dependent degradation of TAB2/3. TRIM38 negatively regulates TLR3-mediated IFN-β signaling by targeting TRIF for degradation.	PMID: 24434549, PMID: 2305647
OAS2		Interferon alpha induced. STAT2/IRF9 directs a prolonged ISGF3-like transcriptional response and antiviral activity in the absence of STAT1. Upon binding to dsRNA or dsDNA, OAS proteins and cGAS produce nucleotide second messengers to activate RNase L and STING (stimulator of interferon genes, gene symbol: TMEM173), respectively; this leads to the initiation of antiviral responses and interferon beta.	PMID: 25564224, PMID: 2575260
SERPING1		C1 inhibitor	PMID: 22576004
IFI44L	c1orf29	Induced by IFNalpha, downregulated by HIV, HIV-1 Vpr induces interferon-stimulated genes in human monocyte-derived macrophages.	PMID: 25170834
IRF8		IRF8 directs stress-induced autophagy in macrophages and promotes clearance of Listeria monocytogenes. IFN Regulatory Factor 8 Represses GM-CSF Expression in T Cells To Affect Myeloid Cell Lineage Differentiation. Negatively regulates plasma cells. Mendelian myco bacteria susceptibility	PMID: 25398936, PMID: 2577503
STX11		Syntaxin11 serves as a t-SNARE for the fusion of lytic granules in human cytotoxic T lymphocytes, Syntaxin-11, but not syntaxin-2 or syntaxin-4, is required for platelet secretion and NK cell de granulation.	PMID: 24227526 , PMID: 2276750
RUNX3		The nuclear receptor nr4a1 controls CD8 T cell development through transcriptional suppression of Runx3. Runt-related transcription factor 3 is involved in the altered phenotype and function in ThPok-deficient invariant natural killer T cells.	PMID: 25762306, PMID: 2456145

SH2D1A		SLAM-SAP signaling promotes differentiation of IL-17-producing T cells and progression of experimental autoimmune encephalomyelitis.	PMID: 25362182
RASSF5		RASSF5 plays an important role in mediating apoptosis in response to death receptor ligands, TNF-α and TNF-related apoptosis-inducing ligand.	PMID: 20810663
ARL4C	ARL7	membrane.	PMID: 21187453
ZNF222			PMID: 25236797
		Phostensin was abundant in helper T-lymphocytes, cytotoxic T-lymphocytes, mature monocytes, macrophages, B-lymphocytes, natural killer cells, and granulocytes.	
PPP1R18		Phostensin binds to the pointed ends of actin filaments and modulates actin dynamics.	PMID: 21804078
PIK3R5		Involved in IL23R/IL17 production.	PMID: 23024273
SELL	CD62L	Marker in t cell colitis transfer model and adoptive therapy for Crohn's.	PMID: 25715355, PMID: 2413216(
		Combined use of biomarkers for distinguishing between bacterial and viral etiologies in pediatric lower respiratory tract infections.	
CD53		Characterization of tetraspanins CD9, CD53, CD63, and CD81 in monocytes and macrophages in HIV-1 .	PMID: 25712729 , PMID: 2357094
BIN2		Cell motility, adhesion and phagocytosis are controlled by actin and membrane remodelling processes.	PMID: 23285027
		p53, nutlin-3-activated ERK1/2 may stimulate the transcription of BCL2A1 via the activation of ELK1, and BCL2A1 expression may contribute to the inhibitory effect of	
BCL2A1		ERK1/2 on nutlin-3-induced apoptosis, thereby constituting a negative feedback loop of p53-induced apoptosis.	PMID: 24867259
TNFSF13B	BAFF	Methylation of TNFRSF13B and TNFRSF13C in duodenal mucosa in canine inflammatory bowel disease and its association with decreased mucosal IgA expression.	PMID: 24814046
SRGN	PPG, PRG, PRG1	Pro apoptosis in DCs.	PMID: 24475103
CMKLR1		Levels are associated with DSS colitis.	PMID: 26265756
SAMSN1	Hacs1	SH3 and SAM domain-containing adaptor protein, is up-regulated by IL-4 in activated B cells and strongly expressed in dendritic cells.	PMID: 21859567, PMID: 1992344
GBP1		Downstream of interferon gamma. Activates T cells.	PMID: 24337748
LINC00847			
RTN1		ER localization and retention. Interacts with HDAC enzymes.	PMID: 17303085, PMID: 2000048
LAIR1		Inhibitory immuno receptor (esp in b cells).	PMID: 24694245, PMID: 1455924
DTNB		Dystrobrevin, scaffold in nucleolus.	PMID: 25959029
PPT1		Identification of palmitoyl protein thioesterase 1 in human THP1 monocytes and macrophages.	PMID: 24083319
		Chronic granulomatous disease (CGD) is a primary immunodeficiency disease that is characterized by susceptibility to bacterial and fungal infections. Various mutations in	
		CYBB encoding the gp91(phox) subunit of the phagocyte nicotinamide adenine dinucleotide phosphate (NADPH) oxidase impair the respiratory burst of all types of	
CYBB	CGD/NOX2	phagocytic cells disrupting the response to IFN-γ.	PMID: 25752509, PMID: 2530178
NOD2		Crohns gene, MDP sensor	PMID:11385577
TIFAB		Negative regulator of TRAF6.	PMID: 19470519
MMP12		Macrophage metalloelastase (MMP12) regulates adipose tissue expansion, insulin sensitivity, and expression of inducible nitric oxide synthase in M2 macrophages.	PMID: 24914938
ADCY7		Macrophages in ADCY7 knock downs produce more TNFa in response to LPS. ADCY7 also affects memory T cells and antibody responses.	PMID: 23229509 , PMID: 1555039
41518			

Table S10: Functional Categories of Genes in TRIM22 Sub network

Functional Categories from NOD2 from TRIM22 vortex:	Correlation within each category (induced by, repressed by pathway signalling or directly modulates)
	ADAR1, CSF2RA,CXCL9, CECR1, PPT1, MMP12, GMFG, ITGB2, SPI1, SLAMF8, Il27RA, PTGES, CSF3R, PTAFR, CD300A, FGR, SLAMF7
Monocyte, Macrophage	EMR2, LILRA5, FCGR3A, GPNMB, HCK, CXCL10, IL10RA, IFI44L, PPP1R18, CD53, TGFB, ADCY7, PLXNC1
Neutrophil	CXCL5, CEBPB, GMFG, CXCL6, FGR, EMR2, TGFB
DCs	CXCL9, SPIB, S1PR4, ITGB2, CLEC4A, KYNU (tolerance), IGSF6, BATF2, CXCL10, IL10RA, SDC3
T effector	
CD4	CSF2RA, ICOS, FAM65B, CD40LG, SPIB, GMFG, RUNX3 (suppression to induce IELs), CDC42SE1, MAP3K8, SELL
CD8/NK	CLEC1A, GZMB, CLEC1A, STX11, RUNX3
T17	PIK3R5, ARID5A, MAP3K8, SH2D1A, CXCL6, CLEC7A, IL41I, SH2D1A
T regulatory	SOCS1, IL4I1, CTLA4, CD274
CD4	PDCD1LG2, CLEC7A, IL27RA, IL2RA, Il10R, DTX1, PPP1R18, TGFB
CD8	LILRB4, IL27RA
B	LAIR1, NFAM1, SPIB, DOK3, IL27RA, IFI30, PPP1R18, ELK2AP
Cytoskeleton (migration & phagocytosis/ immunological synapse/ mechanics	CDC42SE1, GBP1P1,PPP1R18, BIN2
migration	FPR3, CXCR6 (ILC), FAM65B, CXCL9, MMP25, GPSM3, PLXNC1, AKAP11, GMFG, LIMS3
Endosomal	SLC15A3, DNAJC5B, SNX10
Complement	C1S, CFP, CFH, SERPING1
Tissue re-modelling/ thrombins	FPR3, MMP19, COL1A1, TIMP1,F2R
E2/E3 ligase, ubiquitin pathway	SENP7, ASB2, UBE2E2, FBXO6, UBE2D1, PDE4B, DTX1
Inflammasome	GPSM3, MNDA, inflammassome (apoptosis), DYSF, GFI1, GBP5
Autophagy	LAP3, DRAM1, TRIM5
Lysosomal	LYST, GPNMB
Platelets	STX11
	CECR1, MX2, PML , PARP9,CD40 , DOK3, BST2, ACP5, PSTPIP2, PTGES, CLEC4A, GBP4, IRF1, GBP1P1, MSANTD3, STAT1, PML, BATI
Viral infection and response (interferon inducible)	APOL1, IL15RA, IFI30, OAS2, IFI44L, SDC3
	LRRC33, NFAM1, TIFAB, GZMB, CYBB, DRAM1, TIFA, TNFRSF6B, BST2, TNFAIP2, NCF2, PTGES, PTAFR, BID (TNFa only, SLAMF7),
NFKB/TNFα/ apoptosis	EMILIN2 (apoptosis), IRF1 (TNFa induced), PLEK,APOL1, SLC2A3, TRIM38, RASSF5, DNASE, APOL2/ BASP1, ADCY7, UBE2D1
ROS/NADPH/ phagosome	CYBB, CYBA, HV1, SLAMF8, NCF2, FGR, NCF4, IFI30
Mycobacteria response (NOD2/IFN synergy (part viral))	SLC15A3, STAT1, CXCL10, IL15RA, NCF4
P53 (same as Trim22)	NCF2, ARHGAP30
Prostaglandin/arachadonic acid	PLA2G7, TBXAS1
Antigen Presentation/ MHC	CIITA, RFX5, LILRB2, CD1E, SCIMP
Miscellaneous Inflammatory (adhesion)/signalling/muscle	GNAI2, CD18, PLA2G4F, CHST2, DTNB, ST3GAL5, GM2A, GNB4, SDC3, PLEKHO2, LIMS3L/ ZYX/ DYSF
Activation	CD86, CD40
Cell cycle/ prolif	CECR1, KDM2B, CENPV, MRAS
Metabolic/lipids	APOC1, APOC1P1, APOE, CCDC71L, VPS13C, KCNAB2, FAH, SLC43A3, NNMT, CP, ARL4C, SLC2A6, APOL4
Misc (biochem)	FTSJD2, NAPSB, GNGT2, ZNF222
IEC/ enteroendocrine	SLC39A4, SPIB, ITPRIP
ER	RTN1

Table S11: Adult and VEO IBD Network Predicted Key Drivers

Adult Key Drivers	Overlap of Adult IBD Key Drivers in 179 gene TRIM22 Subnetwork
CYYR1	TRIM22
ZNF521	EMR2
INSR	CLEC7A
GLCCI1	CYBB
CREB5	CEBPB
ASAP1	IL10RA
LOC100132891	ITGB2
HIP1	TNFSF13B
ST3GAL1	UBE2E2
DOCK8	DNASE2
TRIM22	GBP4
EMR2	LAP3
C1R	PLXNC1
MMP14	CLEC4A
PMAIP1	GZMB
KIF26B	CXCL9
IL8	RUNX3
BTN2A2	MMP19
FPR2	CD86
LOC100505687	FGR
PDE4A	TIFA
LDHB	KYNU
KLHDC7B	NFAM1
OAS2	PPP1R18
COL1A1	CXCL6
NCF1C	STX11
DARC	MRAS
TMTC1	SERPING1
HLA-DPA1	CD53
GJD3	SAMSN1
SLAMF8	CTLA4
CCR1	TLR8
C9orf91	DYSF
CRLF3	DRAM1
TNS1	STAT1
CDK14	IGSF6
CYBB	GBP1
IL13RA2	CCDC71L
CXCL10	MX2
RAMP2	RASSF5
FSCN1	BID
FCN3	GMFG
SELE	OAS2
ITGAM	COL1A1

ME1	SLAMF8
ABLIM3	CXCL10
CD37	TNFAIP2
FNDC3B	BCL2A1
CSGALNACT2	PLA2G7
INHBA	NCF2
PHACTR1	SOCS1
EMR1	SLC2A6
PPM1F	SELL
ASPHD2	LAIR1
S1PR3	CXCL5
WNT5A	ST3GAL5
SFRP2	LILRB4
VWF	ICOS
TNFAIP2	GM2A
SMARCB1	MNDA
FBN1	CSF2RA
CNN2	BASP1
MAFB	
BCL2A1	
MAPK1	
BST2	
IL10RA	
IFI44	
ARHGAP15	
GRHL1	
C17orf96	
CDC42BPG	
GPX8	
STEAP4	
TPP1	
TRPM6	
GIMAP7	
PIP4K2A	
FLJ43663	
PIK3R3	
HERC5	
ENTPD1	
ITGB2	
ADAMTS2	
DUSP10	
GPRIN2	
ADAM19	
TNFSF13B	
MLKL	
GAS7	

COL5A1
HCK
WHAMMP2
IL23A
OSMR
PLA2G7
FCGR2A
ITGA4
SLC7A11
FLI1
C4orf32
TREM1
HTRA1
NFKBIA
CDX2
NPEPL1
NCF2
CCL8
FPR1
UBE2E2
CD80
CD300LF
RNF166
GAD1
GCA
THBS2
IL6
PKHD1L1
SOCS1
ADAMTS5
ERG
LOC100506941
IL1R1
GIMAP2
LAP3
SNX20
TBL1X
ST8SIA4
PLXNC1
DOCK2
GABBR1
EBI3
SLC22A15
CLYBL
ADAMTS1
TBC1D9

CCL11
PTGS1
CLEC4A
PFKFB3
GPR4
HSD11B1
PEA15
HSH2D
RBPMS
TNFSF4
ANKRD44
LCP2
LAMP3
AGTRAP
ARHGAP20
CH25H
SLC6A14
IL12RB1
MCAM
GLUL
IER3
TLR2
TGIF2
RGS1
EGFL6
SLC2A6
CXCL9
UCP2
RUNX3
GAS1
IL1B
SLC9B2
ZNF618
CXCL11
IL1RAP
BICC1
PDZK1IP1
SEMA4A
FCGR1A
CTGF
KMO
CLIC2
RHOQ
CAV1
TICAM2
TNFAIP6

SELP
SOCS3
SLC16A6
RGS5
IFITM2
SELL
IFITM1
IL11
LAIR1
CD86
CYP27B1
C1orf162
LSP1
SLC25A23
EVI2B
FKBP11
TSPAN2
DENND3
AKT3
TIFA
GPR68
FCGR2B
FYB
ARMCX1
PIK3CD
KYNU
RAPGEF6
IL33
CACNA2D1
SLC1A3
TNF
ITPR1
CCL18
CXCL5
CXCL1
ST3GAL5
GPR183
CHI3L1
TMEM154
NINJ2
HLA-DOB
GJA5
FCHSD2
ORAI2
F5
NPL

PRDM1
KCNJ15
CCDC3
CHRDL2
TPST1
LAMC1
TYROBP
ZNF331
SLC9A1
MXRA5
CXCL6
GZMK
COL5A2
CLIP4
DOCK10
LIX1L
MIR155
IGDCC4
LILRB4
GJA1
ROBO4
DENND5A
CKAP2
LHFP
IL18R1
PEAR1
MRAS
SERPING1
ARHGAP39
IFITM3
CFI
TDO2
EDNRA
CD53
EHD3
CXCR2
ABCA1
KIAA1199
CDH11
EOMES
S100B
IL1RN
RASA3
PAPLN
SLFN11
ST6GAL1

SAMSN1
CYP26B1
STC1
CD180
ICOS
MLK7-AS1
CTLA4
C13orf44-AS1
CD79A
LAMP5
WNK3
GM2A
IDO1
FAM20A
LOC648987
DISC1
FAM110B
ANKRD55
TSHZ2
TWIST2
DDR2
LRRK2
STAT1
IGSF6
PPM1M
SLC2A14
RILPL2
SASH3
IRS1
GBP1
CCDC71L
MMP3
PDE10A
COL15A1
LINC00152
TTC7B
MX2
SCRN1
ITGAX
SCUBE2
LAIR2
IL4I1
CD300C
TSPAN4
FCER1G
RASSF5

GBP2
MNDA
CD109
BID
CSF2RA
B9D1
CHST15
GMFG
ACSL4
RGS10
CLIC4
VNN2
LITAF
PECAM1
GPR176
COL1A2
LPAR6
LY96
VEGFC
NOS2
CD84
EMID1
CLIC6
TRIB2
CTSK
PDPN
TMEM45A
HAVCR2
CLEC7A
MCL1
PTPN11
CTHRC1
RNF24
AKAP1
DUOXA2
MAT2A
LST1
NR4A3
CXCR1
CEBPB
CCL4
APCDD1
IRAK3
CD48
DUOX2
ALOX5AP

MMP1
QPCT
HAPLN3
ZEB1
TBC1D4
TNFSF11
RHOH
MS4A1
SNN
FGF7
SULF1
GPR116
PRNP
SERPINE1
KRT23
OLFML2B
TRDV3
DAZAP2
SERPINI1
PXDN
DNASE2
IL7R
C12orf5
ESAM
WISP1
ACSL1
WBP5
GBP4
TESC
CCL3
RASSF2
SLC15A3
DUSP6
COL4A1
C4BPB
FCRL1
CCL2
LOC100129518
GZMB
CLEC4D
SERPINB5
SEMA4D
KLRF1
JAZF1
ZNF277
CYSLTR1

LIN7A
CD83
LOC100652805
MMP19
EVI2A
TRERF1
GNA12
FGR
IPCEF1
SPP1
C5AR1
CEP170
SAMD3
LMBR1
SALL1
MMP10
ATP6AP2
KIRREL
NFAM1
JAK3
GZMH
CFP
CMTM2
COG1
PPP1R18
ADRBK2
STX11
SELT
FAM26F
RHOA
RAB8B
TANK
SLC28A2
GIMAP1-GIMAP5
STEAP1B
MYEOV
ZG16
AIDA
VNN3
C13orf44
IGHA1
TLR8
DYSF
IFIT1
BASP1
KCNJ10

SUPPLEMENTAL MATERIALS FOR:

Variants in *TRIM22* that Affect NOD2 Signaling Are Associated With Very Early Onset Inflammatory Bowel Disease

Qi Li[1,2,§,*], Cheng Hiang Lee[3,4,§,*], Lauren A Peters[5,6,*], Lucas A Mastropaolo[2,§,#], Cornelia Thoeni[1,2,§,#], Abdul Elkadri[1,2,7,#,§], Tobias Schwerd[8,#], Jun Zhu[6], Bin Zhang[6], Yongzhong Zhao[6], Ke Hao[6], Antonio Dinarzo[6], Gabriel Hoffman[6], Brian A Kidd[6], Ryan Murchie[1,2,§], Ziad Al Adham[1,2,7,§], Conghui Guo[2,§*], Daniel Kotlarz[9], Ernest Cutz[10], Thomas D Walters[1,2,§], Dror S Shouval[11,§], Mark Curran[12], Radu Dobrin[12], Carrie Brodmerkel[12], Scott B Snapper[11,13], Christoph Klein[9], John H Brumell[1,7,14§], Mingjing Hu[3,4], Ralph Nanan[3,4], Brigitte Snanter-Nanan[3,4], Melanie Wong[15], Francoise Le Deist[16], Elie Haddad[17], Chaim M Roifman[18], Colette Deslandres[19], Anne M Griffiths[1,2,§], Kevin J Gaskin[3,4], Holm H Uhlig[8], Eric E Schadt[6,%], Aleixo M Muise[1,2,7,§, % ^]

Table of Contents

Supplemental Figures

References

Methods

Subjects: All experiments were carried out with the approval of the Research Ethics Board (REB) at the Hospital for Sick Children. Informed consent to participate in research was obtained. A copy of the consent is available on the interNational Early Onset Pediatric IBD Cohort Study (NEOPICS) website at http://www.neopics.org/NEOPICS_Documents.html.

Genetics

Whole exome sequencing: For patient 1 and her parents (trio), whole exome sequencing (WES) was performed using the Agilent SureSelect Human All Exon 50Mb kit with high-throughput sequencing conducted using the SOLiD 4 System at The Center for Applied Genomics (TCAG) through the Hospital for Sick Children (Toronto, ON). Sanger sequencing was used to verify variant genotypes in the Family 1 and infantile patients from the collaborating institutions were screened for *TRIM22* variants.

Analysis: Whole exome sequencing of Patient 1 and her parents resulted in greater than 100 times mean exome coverage and identified 152,020 variants. Using SNP and Variation Suite Version 8.1 (Golden Helix), variant call files (VCF) were organized by the family pedigree. Using the 1000 genomes Variant Frequencies (Phase 1) and the NHLBI Exome Sequencing Project V2 Exome Variant Frequencies, rare variants with a minor allele frequency below 1% were filtered. This resulted in 16,097 rare variants. Variants were then selected based upon whether they were deemed to be coding. From this list, we then identified 12 non-synonymous homozygous variants (Table S2) that were inherited in an autosomal recessive manner. Non-synonymous and unclassified variants were then scored using the database for non-synonymous functional predictions (dbNSFP 2.9), filtering out variants found to have no damaging score (Polyphen2, SIFT, MutationTaster, MutationAssessor, FATHMM). As well, variants were scored using PhyloP and GERP++ to determine conservation (Figure S1). Based on known protein function, expression profiles, animal models, mutation conservation, and network analysis, this list was narrowed down to a single candidate variant in *TRIM22*.

Validation: In order to validate these findings, we examined WES results from 150 infantile international VEOIBD patients without a genetic diagnosis who were previously sequenced in Toronto (NEOPICS), Oxford, and Munich (Care-For-Rare) and did not identify predicted damaging variants in the *TRIM22* gene. Therefore, we performed targeted exome sequencing of the *TRIM22* gene in ten *IL10RA/B*, and *IL10* negative patients without previous WES, and identified two additional patients with *TRIM22* variants (Patients 2 and 3) with a very similar severe phenotype of granulomatous colitis and severe perianal disease.

Computational Analysis

Dataset: Blood and biopsy data was collected at baseline from anti-TNF resistant CD patients enrolled in the Ustekinumab trial previously described[1]. Two 2.5 mL blood samples were collected at the trial baseline using PAXgene tubes from all subjects (1528 blood samples in total). All blood samples were stored at -80°C until RNA isolation was performed. A subset of 150 blood samples was hybridized by microarray for genome-wide mRNA expression profiling. Ileal, rectal, and colonic biopsies were collected at the screening visits from a sub-group of

subjects who consented to this procedure. Biopsies were obtained from selected colonic sections, including the ascending, transverse, and descending colonic regions, and from both inflamed and non-involved areas. The inflamed regions were defined as the colonic segments with the most severe disease activity. Additional biopsies were collected from the terminal ileum and from the rectum (i.e., the distal 10 cm of the colon).

Total RNA including micro ribonucleic acids (miRNA) was isolated with PAXgene Blood RNA MDx Kit plus customized reagent BM3 (Qiagen Inc., Valencia, CA). RNA quantity and quality were determined with a LabChip GX (Caliper Life Sciences, Hopkinton, MA). Gene expression were carried out using Affymetrix GeneChip HTHGU133+ (Affymetrix, Santa Clara, CA, Cat# 901262) according to the manufacturer's protocol with the exception that DMSO replaced the Tetramethylammonium Chloride Solution (TMAC) in the hybridization buffer. Arrays were washed and stained on the Affymetrix GeneChip Array Station then scanned on an HTAPS scanner.

Reconstruction of the Bayesian Networks: Bayesian networks are directed acyclic graphs in which the edges of the graph are defined by conditional probabilities that characterize the distribution of states of each node given the state of its parents. The network topology defines a partitioned joint probability distribution over all nodes in a network, such that the probability distribution of states of a node depends only on the states of its parent nodes: formally, a joint probability distribution $p(X)$ on a set of nodes X can be decomposed as $p(X) = \prod_i p(X^i \mid \mathrm{Pa}(X^i))$, where $\mathrm{Pa}(X^i)$ represents the parent set of X^i. In our networks, each node represents transcription expression of a gene. These conditional probabilities reflect not only relationships between genes, but also the stochastic nature of these relationships, as well as noise in the data used to reconstruct the network.

Bayes formula allows us to determine the likelihood of a network model M given observed data D as a function of our prior belief that the model is correct and the probability of the observed data given the model: $P(M \mid D) \propto P(D \mid M) * P(M)$. The number of possible network structures grows super-exponentially with the number of nodes, so an exhaustive search of all possible structures to find the one best supported by the data is not feasible, even for a relatively small number of nodes. We employed Monte Carlo Markov Chain (MCMC) [2] simulation to identify potentially thousands of different plausible networks, which are then combined to obtain a consensus network (see below). Each reconstruction begins with a null network. Small random changes are then made to the network by flipping, adding, or deleting individual edges, ultimately accepting those changes that lead to an overall improvement in the fit of the network to the data. We assess whether a change improves the network model using the Bayesian Information Criterion (BIC)[3], which avoids over fitting by imposing a cost on the addition of new parameters. This is equivalent to imposing a lower prior probability $P(M)$ on models with larger numbers of parameters.

Even through edges in Bayesian networks are directed, we can't infer causal relationships from the structure directly in general. For example, in a network with two nodes, X^1 and X^2, the two models $X^1 \to X^2$ and $X^2 \to X^1$ have equal probability distributions as $p(X^1, X^2) = p(X^2 \mid X^1)\, p(X^1) = p(X^1 \mid X^2)\, p(X^2)$. Thus, by data itself, we can't infer whether X^1

is causal to X^2, or vise versa. In a more general case, a network with three nodes, X^1, X^2, and X^3, there are multiple groups of structures that are mathematically equivalent. For example, the following three different models, $\mathrm{M1}: X^1 \to X^2, X^2 \to X^3$, $\mathrm{M2}: X^2 \to X^1, X^2 \to X^3$, and $\mathrm{M3}: X^2 \to X^1, X^3 \to X^2$, are Markov equivalent (which means that they all encode for the same conditional independent relationships). In the above case, all three structures encode the same conditional independent relationship, $X^1 \not\perp X^3 \mid X^2$, X^1 and X^3 are independent conditioning on X^2, and they are mathematically equal.

$$\begin{aligned} p(X) &= p(\mathrm{M1} \mid D) = p(X^2 \mid X^1)\,p(X^1)\,p(X^3 \mid X^2) \\ &= p(\mathrm{M2} \mid D) = p(X^1 \mid X^2)\,p(X^2)\,p(X^3 \mid X^2) \quad . \\ &= p(\mathrm{M3} \mid D) = p(X^2 \mid X^3)\,p(X^3)\,p(X^1 \mid X^2) \end{aligned}$$

Thus, we can't infer whether X^1 is causal to X^2 or vise versa from these types of structures. However, there is a class of structures, V-shape structure (eg. $\mathrm{Mv}: X^1 \to X^2, X^3 \to X^2$), which has no Markov equivalent structure. In this case, we can infer causal relationships. There are more parameters to estimate in the Mv model than M1, M2, or M3, which means a large penalty in BIC score for the Mv model. In practice, a large sample size is needed to differentiate the Mv model from the M1, M2, or M3 models.

Incorporating genetic data as a structure prior in the Bayesian network reconstruction process: In general, Bayesian networks can only be solved to Markov equivalent structures, so that it is often not possible to determine the causal direction of a link between two nodes even through Bayesian networks are directed graphs. However, the Bayesian network reconstruction algorithm can take advantage of the experimental design by incorporating genetic data to break the symmetry among nodes in the network that lead to Markov equivalent structures, thereby providing a way to infer causal directions in the network in an unambiguous fashion[4]. We modified the reconstruction algorithm to incorporate eSNP data as priors as follows: genes with cis-eSNP[5] are allowed to be parent nodes of genes without cis-eSNPs, but genes without cis-eSNPs are not allowed to be parents of genes with cis-eSNPs, $p(trans->cis) = 0$. We have shown that integrating genetic data such as cis-acting eSNP or eQTLs (excluding edges into certain nodes) improves the quality of the network reconstruction by simulations[6] and by experimental validations[4, 7]. We note that in applying this particular version of the Bayesian network reconstruction algorithm (incorporating genetic information as a prior), if genetic information is not available or is ignored, the population is simply treated as a population with random genetic perturbations.

Averaging network models: Searching optimal BN structures given a dataset is an NP-hard problem. We employed an MCMC method to do local search of optimal structures as described above. As the method is stochastic, the resulting structure will be different for each run. In our process, 1,000 BNs were reconstructed using different random seeds to start the stochastic reconstruction process. From the resulting set of 1,000 networks generated by this process, edges that appeared in greater than 30% of the networks were used to define a consensus network. A 30% cutoff threshold for edge inclusion was based on our simulation study[6], where a 30% cutoff yields the best tradeoff between recall rate and precision. The consensus network resulting from

the averaging process may not be a BN (a directed acyclic graph). To ensure the consensus network structure is a directed acyclic graph, edges in this consensus network were removed if and only if (1) the edge was involved in a loop, and (2) the edge was the most weakly supported of all edges making up the loop.

Bayesian network for individual co-expression module: Searching optimal BN structures given a dataset is an NP-hard problem. The computational complexity of our MCMC method for described above is $O(N^4)$, where N is the number of nodes included in the network reconstruction process. It is practically impossible to construct a global Bayesian network including all 39,000 genes from the intestinal tissue. Following the procedure described above, 1,000 BNs were reconstructed using different random seeds to start the reconstruction process. From the resulting set of 1,000 networks generated by this process, edges that appeared in greater than 30% of the networks were used to define a consensus network. Our previous simulation study shows that the 30% inclusion threshold results in a stable structure and achieves the best tradeoff between precision and recall[6]. The histogram of percentage of occurrences of all potential edges shows that 30% is a reasonable cutoff threshold for inclusion (a typical histogram is shown in Figure here).

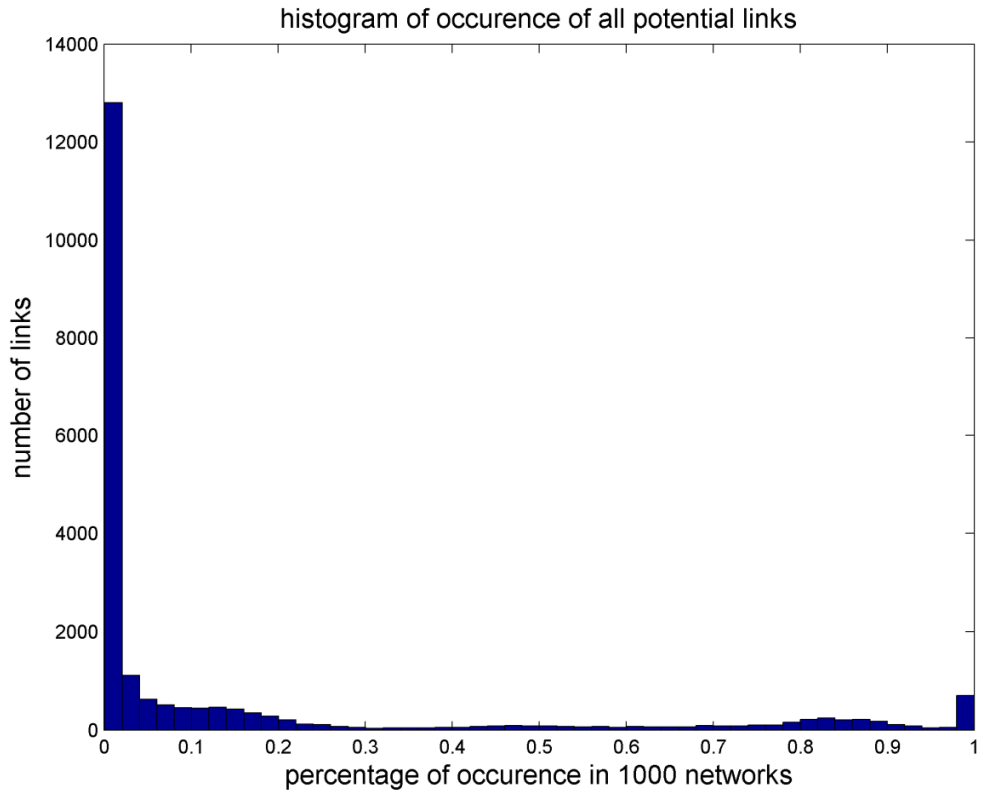

Identification of Key Causal Regulators: For each Bayesian network, we further identified the regulators by examining the number of N-hob downstream nodes (NHDN) for each gene in the directed network[8]. For a given network, let μ be the numbers of N-hop downstream nodes and d be the out degrees for all the genes. The genes with the number of N-hop downstream nodes

(NHDN) greater than $\bar{\mu} + \sigma(\mu)$ are nominated as causal regulators. The regulators with degree above $\bar{d} + 2\sigma(d)$, where d denote the number of downstream genes, become key causal regulators of a corresponding sub-network associated with disease status. These criteria identified genes with number of downstream nodes and number of out links significantly above the corresponding average value. This method was performed on the IBD RISK network to determine VEOIBD Key Causal Regulators.

Weighted Gene Coexpression Network Analysis: The weighted network analysis begins with a matrix of the Pearson correlations between all gene pairs, then converts the correlation matrix into an adjacency matrix using a power function f(x)=x^β. The parameter β of the power function is determined in such a way that the resulting adjacency matrix (i.e., the weighted co-expression network) is approximately scale-free. To measure how well a network satisfies a scale-free topology, we use the fitting index[9] (i.e., the model fitting index R2 of the linear model that regresses log(p(k)) on log(k) where k is connectivity and p(k) is the frequency distribution of connectivity). The fitting index of a perfect scale-free network is 1. For this dataset, we select the smallest β which leads to an approximately scale-free network. The distribution p(k) of the resulting network approximates a power law: $p(k) \sim k^{-\gamma}$.

To explore the modular structures of the co-expression network, the adjacency matrix is further transformed into a topological overlap matrix[9]. As the topological overlap between two genes reflects not only their direct interaction, but also their indirect interactions through all the other genes in the network, previous studies[9, 10] have shown that topological overlap leads to more cohesive and biologically meaningful modules. To identify modules of highly co-regulated genes, we used average linkage hierarchical clustering to group genes based on the topological overlap of their connectivity, followed by a dynamic cut-tree algorithm to dynamically cut clustering dendrogram branches into gene modules[11]. To distinguish between modules, each module was assigned a unique color identifier, with the remaining, poorly connected genes colored grey.
To examine how each gene module was related to clinical traits we first performed principal component analysis for each module, and then computed module-trait correlation between the first principal component (module eigengene) and each trait[12]. The significance (p value) of each correlation was also calculated.

Key Driver Analysis: Key driver analysis (KDA) takes as input a set of genes (G) and a directed gene network N (eg Bayesian network)[12-15]. The objective is to identify the key regulators for the gene sets with respect to the given network. KDA first generates a sub-network N_G, defined as the set of nodes in N that are no more than h-layers away from the nodes in G, and then searches the h-layer neighborhood (h=1,..,H) for each gene in N_G ($HLN_{g,h}$) for the optimal h*, such that

$$ES_{h^*} = \max(ES_{h,g}) \forall g \in N_g, h \in \{1..H\}$$

where $ES_{h,g}$ is the computed enrichment statistic for $HLN_{g,h}$.
A node becomes a candidate driver if its HLN is significantly enriched for the nodes in G. Candidate drivers without any parent node (i.e., root nodes in directed networks) are designated as global drivers and the remaining are local drivers.

Key Driver Analysis was performed by projecting Inflamed Sigmoid and Inflamed Rectum signatures on the Bayesian Ileum network constructed from the ustekinumab trial data.
Differential Expression: Whole-genome transcriptional expression data were collected from

biopsy tissue samples and whole blood of individuals in the Janssen ustekinumab trial (T26). We wanted to identify differential expression signatures of disease status, degree of tissue inflammation (inflamed versus non-involved).

Sample Selection and Data Curation

Biopsy data: A total of 321 biopsy tissue samples were collected from 86 individuals (mean of 4 samples from differential anatomical regions of the terminal ileum, colon, and rectum per individual) at the screening time point of the study. Whole-genome expression data were collected on the Affymetrix ht_hg-u133_pm_ap platform, which contains 54,715 probes (_21,000 genes). Pre-processing of expression data included background correction, log2 transformation, quantile normalization, and Robust Multi-array Averaging to stabilize the variance and rescale the levels across arrays1. Further quality control measures of clustering and principal component analysis (PCA) were employed to identify potential outliers in the data. Age and gender adjustments to expression levels were performed on each tissue location using robust linear regression. Only samples with valid age and gender data were used for analysis.

Blood data: A total of 836 blood samples were collected from 275 individuals during the course of the trial. Whole-genome expression data were collected on the Affymetrix ht_hg-u133_pm_ap platform, which contains 54,715 probes (21,000 genes). Pre-processing and quality control steps were similar to biopsy procedures listed above. Expression levels were adjusted by age, gender, and batch using robust linear regression. Only samples with valid age and gender data were used for analysis.

To identify differential expression signatures, we used an unbiased univariate filter to select top-varying genes and then applied significance analysis of microarrays (SAM)[16] to whole-genome expression data collected from biopsy tissue samples and whole blood of individuals in T26 trial. To control for multiple hypothesis testing, we used the Benjamini & Hochberg adjustment on the raw p-values to control the family-wise error rate, and set a false discovery rate threshold of 1% or 5%. All analyses performed using the R statistical package, version 2.15.24.1.

Comparisons: Biopsy – anatomical region and inflammatory signatures.
To ascertain tissue-specific signatures, we examined inflamed versus non-involved tissue from differential anatomical regions of the small intestine, colon, and rectum.

Clinical variable correlation: We used Spearman correlation to examine the relationship between the mRNA expression of TRIM22 in intestine and blood and several key IBD traits. The correlation test was performed with the R function “corr.test”. We applied a simple Bonferroni correction to a 0.01 significance level across all gene-trait correlation tests performed.

Functional Studies

Constructs: HA-epitope tagged mammalian expression plasmids for NOD1 and NOD2 were obtained from Dr. Dana Philpott (University of Toronto), GFP-tagged Ubiquitin was obtained for Dr. John Brumell (University of Toronto), HA-tagged K48 Ubiquitin and HA-tagged K63 Ubiquitin were obtained for Dr. Jane McGlade (University of Toronto), FLAG-tagged MAVS and FLAG-tagged RIP2 were obtained for Dr. Hong-bing Shu (Wuhan University) and

mammalian expression plasmids for FLAG-tagged TRIM22 and its mutants were constructed by site-directed mutagenesis.

Transfection and Luciferase Reporter Assays: NF-κB luciferase reporter plasmids (Promega) and ISRE promoter and IFNβ promoter luciferase reporter plasmids were obtained from Dr. Hong-bing Shu (Wuhan University). A total of HEK 293 cells (1×10^5) were seeded on 24-well dishes and transfected the following day using Lipofectamine 2000 method. Empty control plasmid was added to ensure that each transfection received the same amount of total DNA. To normalize for transfection efficiency, 0.01μg of pRL-TK (Renilla luciferase) reporter plasmid was added to each transfection. Approximately 24h after transfection, luciferase assays were performed using a dual-specific luciferase assay kit (Promega). Firefly luciferase activities were normalized on the basis of Renilla luciferase activities. Cells were treated with recombinant TNFα, RSV, or L18-MDP (InvivoGen). Statistical analysis of luciferase assay data consisted of two-way ANOVA followed by Bonferroni post-hoc testing to compare across conditions. Statistical significance was assigned to tests with $p<0.05$ after Bonferroni correction.

Quantitative real-time PCR: Total RNA was isolated from cells using Trizol reagent (Ambion), reverse-transcribed in cDNA using Superscript VILO (Invitrogen), and subjected to qPCR analysis to measure mRNA expression levels of tested genes. Gene-specific primer sequences were as follow: *ISG15*: 5′-AATGGGCTGGGACCTGACGG-3′ (forward), 5′-TTAGCTCCGCCCGCCAGGCT-3′ (reverse); *IL-6*: 5′- CCT GAACCTTCCAAAGATGGC-3′ (forward), 5′-TTCACCAGGCAA GTCTCCTCA-3′ (reverse); *TNF*: 5′-GAGGCCAAGCCCTGGTATG-3′ (forward), 5′-CGGGCCGATTGATCTCAG C-3′ (reverse); *GAPDH*: 5′-GAGTCAACGGATTTGGTCGT-3′ (forward), 5′-GACAAGCTTCCCGTTCTCAG-3′ (reverse). Statistical analysis of qPCR data consisted of two-way ANOVA followed by Bonferroni post-hoc testing to compare across conditions. Statistical significance was assigned to tests with $p<0.05$ after Bonferroni correction.

Coimmunoprecipitation and Immunoblot Analysis: For transient transfection and coimmunoprecipitation experiments, HEK 293 cells (1×10^6) were seeded for 24 hr then transiently transfected for 18–24 hr using Lipofectamine 2000 according to the manufacturer's protocols. Transfected cells were lysed in 1 mL of lysis buffer (150mM NaCl, 50mM HEPES, 1% Triton X-100, 10% glycerol, 1.5mM $MgCl_2$, 1.0mM EGTA) supplemented with protease and phosphatase inhibitors (aprotinin (1:1000), leupeptin (1:1000), pepsin (1:1000) and, PMSF (1:100). For each immunoprecipitation, a 0.9mL aliquot of the lysate was incubated with 0.5 μg of the indicated antibody and 40 μL of a 1:1 slurry of Protein G Sepharose (Bioshop) for 1 h. Sepharose beads were washed 3X with 1 mL of high salt lysis buffer containing 0.5 M NaCl. The precipitates were analyzed by standard immunoblot procedures using the following antibodies: mouse monoclonal anti-FLAG (Sigma), anti-HA (Origene), anti-NOD2 (Novus), anti-GFP (Invitrogen), rabbit polyclonal anti-TRIM22 (Abnova) and goat polyclonal anti-NOD2 (Ingenix). For endogenous coimmunoprecipitation experiments, HT29 cells (5×10^7) were stimulated with MDP (10μg/mL) for the indicated times or left untreated. The coimmunoprecipitation and immunoblot experiments were performed as described above.

shRNA Transduced Stable HT29 cells: shRNA targeted to TRIM22 was obtained from Dr. Barr's lab (University of Western Ontario). The HT29 cells were transfected with two packaging

plasmids, pMD2G and pSPA, and the GFP control or TRIM22 shRNA retroviral plasmid by calcium phosphate precipitation. Cells were washed 12 hr after transfection and new medium without antibiotics was added for 24 hr. The recombinant virus-containing medium was filtered and used to infect HT29 cells in the presence of polybrene (4µg/mL). The infected HT29 cells were selected using puromycin (2µg/mL) for 2 weeks before additional experiments were performed.

Immunohistochemistry: Colonic biopsies and tissues from colon resection specimen were fixed in 10% neutral buffered formalin and embedded in paraffin. Sections cut at 5 µm were placed on Superfrost Plus (Fisher Scientific, Waltham, MA) microscope slides. Following incubation at 60°C for 30 min, the tissues sections were deparaffinized and rehydrated using sequential washes (100% xylenes, 5 min x 2; 50% xylenes: 50% ethanol, 5 min; 100% ethanol, 5 min x 2; 95% ethanol, 3 min; 75% ethanol, 3 min; 50% ethanol, 3 min; cold H_2O, 5 min). Sections were then stained with haematoxylin and eosin (H&E) for 10 min, followed by sequential washes in cold H_2O. Stained tissue was mounted using xylene based mounting media. Stained sections were photographed with a Nikon Light Microscope and adjusted for brightness and contrast using Adobe Photoshop.

Fluorescent Confocal Microscopy

Immunofluorescence on biopsy samples: Paraffin sections were deparaffinized using xylene and rehydrated in ethanol at different concentrations. Antigen retrieval was performed using high pressure-cooking in EDTA buffer, pH 9. Afterwards tissue sections were blocked for 1 hr at RT with 5% BSA and 15% goat serum in 1X PBS without Ca2+ and Mg2+ to avoid nonspecific antibody binding. First antibody incubation was performed overnight at 4°C. Next day, sections were washed 3X for 10 min with 1X Ca2+, Mg2+ free PBS. Tissue slides were incubated with secondary antibody for 1 hr in darkness at RT and afterwards washed 3X for 10 min with 1X PBS without Ca2+ and Mg2+. Finally mounting of stained sections were performed overnight using Vectoshield Mounting Medium. Polyclonal rabbit anti-TRIM22 (Sigma Aldrich), monoclonal mouse anti-NOD2 (Novus Biologicals), polyclonal rabbit anti-Flag (Sigma Aldrich) and mouse monoclonal HA (Thermo Scientific) were used as first antibodies in a 1:100 dilution. ALEXA 488 goat anti-mouse and ALEXA 568 goat anti-rabbit were used as secondary antibodies at a dilution of 1:500. Nuclei were stained using Dapi (Thermo Scientific) in a dilution 1:10 000. Images of stained slides were taken on an Olympus Spinning disk confocal microscope and adjusted for brightness and contrast in the Velocity Software 6.1.1.

Peptide inhibition of NOD2 in human biopsy samples: NOD2 peptide (ab39813, Abcam) was incubated overnight at 4°C with the NOD2 antibody (ab36836, Abcam) in the following proportion: 10X peptide concentration to 1X antibody. Next day immunofluorescence analysis on biopsy samples was performed as described above.

Immunofluorescence on HEK 293 cells: Cells were fixed in 4% paraformaldehyde and permeablized with 0.01% Triton-X-100 for 1 minute. Blocking was performed at RT for 1 hour and first antibody incubation overnight at 4°C. Afterwards cells were washed 3X for 10 minutes with 1X PBS without Ca2+ and Mg2+. Next cells were incubated with secondary antibodies for 1 hr at RT in darkness, washed 3X for 10 minutes with 1X PBS without Ca2+ and Mg2+ and

finally mounted with Dako Fluorescent Mounting Medium (Dako). Nuclei counter-staining as well as first and secondary antibodies were the same as used for biopsy staining.

Intracellular TNF staining and flow cytometry: Peripheral blood mononuclear cells (PBMCs) were isolated by gradient centrifugation from whole blood from patient, parent or healthy donor. NOD2-dependent TNF response in monocytes was evaluated as previously described (please cite PMID 24611904). In brief, PBMCs were cultured overnight in RPMI1640 supplemented with 10% FCS. The following day, cells were gently washed with PBS and activated for 2.5 hours with 200 ng/ml L18-MDP (Invivogen) or 200 ng/mL LPS (Enzo) in the presence of Golgiplug (BD Bioscience). After stimulation, cells were harvested by scraping, put on ice and labelled with fixable viability dye (eBioscience) and surface monocyte markers. Following fixation and cell permeabilization (Cytofix/Cytoperm Kit, BD Bioscience) cells were stained for intracellular production of TNF. The following antibodies were used: anti-TNF (clone MAb11, eBioscience), anti-CD14 (clone M5E2) and anti-HLA-DR (clone L243, both BioLegend). Results were acquired by flow cytometry (LSRFortessa, BD Biosciences) and data analyzed with FlowJo software (Version 10.0.6, Treestar).

Detailed Case Reports – Patients 1 to 3

Patient 1: Patient 1 was born at term with a birth weight of 3.8 kg to consanguineous parents of Lebanese descent. At 8 days old, she presented with fever, poor feeding, mouth ulcers, diarrhea, and perianal excoriation. Chest X-ray showed increase opacity over right upper zone, consistent with right upper lope collapse. She was treated with empiric antibiotics and started on amino acid based formula for presume cow's milk protein allergy. During the next few months, she had recurrent fever, mouth ulcers and poor feeding.

At 7 months old, Patient 1 experienced severe pain associated with defecation and bloody diarrhea. She was later referred for investigation of possible VEOIBD. Clinical examination revealed multiple perianal skin tags and fissures. Colonoscopy showed active chronic proctitis with granuloma formation. She was treated with prednisolone leading to some symptomatic relief, however she later proved to be steroid dependent. Gastrostomy was inserted at 9 months to facilitate continuous feed in view of her significant growth failure.

Infliximab was started at 16 months old but she developed anaphylaxis after 2 doses. As her perianal disease deteriorated, she experienced very severe pain while defecating. In order to reduce fecal output and hence reduce the perianal symptoms, she was commenced on 6 months of total parenteral nutrition (TPN) with complete gut rest. She remained symptomatic despite these interventions.

Simultaneously, Patient 1 also had partial upper airway obstruction with non-granulomatous inflammatory polyps in the pharynx; these were removed surgically. After the upper airway obstruction was resolved, Adalimumab was introduced with no clinical improvement. Subsequently, her course was punctuated by multiple infections, even though screening tests for immunodeficiency were normal (discussed below).

At 25 months old, a diversion colostomy was performed to control her perianal disease. Initially there were marked improvements after fecal stream diversion and topical tacrolimus treatment. However she continued to have colitis and poor growth.

At 3 years old, she developed fistulae around her colostomy site. Due to persistent disease, she had sub-total colectomy and formation of end ileostomy at 4 years old.

At nearly 5 years old, Patient 1 had type-2 respiratory failure secondary to Coronavirus respiratory tract infection. Further investigation revealed that she had severe bronchiectasis, probably secondary to recurrent respiratory tract infection.

Presently, the combination of supplementary parental nutrition, fecal stream diversion and no immunosuppressive medication, Patient 1 has been relatively symptom free with appropriate growth.

She had numerous central venous access associated sepsis; *Candida parapsilosis*, *Enterobacter cloacae*, *Coagulase negative staphylococcus*, pseudomonas aeruginosa, *Escherichia coli*, *Klebsiella oxytoca* were cultured in her blood. She also had multiple respiratory infections, microorganism isolated included *Respiratory syncytia virus*, *Influenza A*, *Coronavirus*, *Human*

metapneumovirus, and *Pseudomonas aeruginosa*. The majority of her infections of viral origin occurred within 48 hours post-Adalimumab injection.

Her immunological workup showed on multiple occasions with ongoing inflammation normal to mildly elevated IgG, IgM, IgE, and IgA. Immunophenotyping showed normal populations of CD3, CD4, CD8, CD4:CD8 ratio, CD19, and NK cells. There was normal expression of CD11b and CD18 compared to normal controls indicating no evidence of leukocyte Adhesion Deficiency Type 1. C3 and C4 levels were noted to be normal. The following antibodies were noted to be negative: Anti-dsDNA, Anti-Myeloperoxidase, Anti-PR3, and Anti-Nuclear Antibody. She was found to have C-Anti-Neutrophil Cytoplasmic Antibody positivity 1/80. NBT testing was normal on several occasions, and Neutrophil Oxidative Burst Index was found to be normal as well. Screening for Familial Mediterranean Fever was found to be negative. Functional studies demonstrated a normal TNFα response to L18-MDP stimulation (data not shown). Whole exome sequencing performed showed no variants within *NOD2*, *IKBKG*, *XIAP* or other genes known to cause primary immunodeficiency or other genes know to cause colitis[17].

Patient 2: Patient 2 was born premature at 35 weeks of gestation to non-consanguineous parents of Jamaican descent. There is a family history of Crohn's disease in his uncle. At 3 ½ months old, he presented with a fever and a rash and was found to have hypoalbuminemia and severe microcytic anemia (hemoglobin of 67 g/l, MVC 60). His septic workup was negative and he was treated with a change in his diet to a semi-hydrolyzed formula.

At 6 months of age, he presented with an acute lower GI bleed and was found to have a major coagulopathy, hypoalbuminemia and severe anemia (69 g/L). During this admission, he developed a perianal abscess on his left gluteal region that was surgically drained. He had multiple infections during this admission (*E. coli* urinary tract infection, Rotavirus and a positive urine culture for CMV). Colonoscopy found large ulcerations in the sigmoid and descending colon with multiple pseudopolypoid lesions and marked background inflammation with loss of vasculature. Biopsy pathology noted inflamed granulation tissue lined by histiocytes and fibrino-purulent exudate. His upper endoscopy was visually normal, but granulomas were noted on patholgoy of the stomach biopsies. He was started on an amino acid formula.

At 9 months old, he presented with polyarthritis and dactylitis. He continued to have severe anemia with elevated acute phase reactants. He was started on steroids and subsequently azathioprine for maintenance therapy.

At 13 months of age, he was admitted with a severe flare of his colitis and a severe drop of his hemoglobin to (39 g/L). Colonoscopy reconfirmed pancolitis. Biopsies showed noncaseating granulomata with changes of chronic colitis. Azathioprine was changed to methotrexate. He also was found to have a perianal abscess on his right buttocks that was drained surgically.

At 18 months, he presented with severe diarrhea resulting in metabolic acidosis requiring admission and rehydration. Prednisone was restarted.

At 20 months, his perianal disease worsened with the development of multiple fistulae. Infliximab was attempted at 4.2 mg/kg/dose.

At 23 months, his perianal disease worsened. Colonoscopy showed again pancolitis with serpigineous ulcers from rectum to proximal descending colon.

At 24 months, he continued to flare and his perianal disease worsened. He was noted to have a loss of response to Infliximab, and he underwent a left-sided colectomy with placement of a colostomy.

He presented again at 28 months with a further ischio-rectal abscess of the right buttock that was drained surgically.

At 38 months, he developed a large peri-colostomy abscess with a generalized worsening of disease. Infliximab was restarted, and he developed an allergic reaction after the second dose. He continued to worsen and subsequently required a right hemicolectomy with ileostomy formation.

Abscess continued to form for the next three years, requiring admission and drainage. Adalimumab was attempted with improvement of weight and symptoms.

As for extra-intestinal manifestations, he has had dactylitis and polyarthropathy since 9 months of age. These have improved on steroid therapy. He also developed orchitis and epididymitis requiring treatment with clavulin. He developed pyoderma gangrenosum near the site of ileostomy.

His initial immune workup noted a normal NBT test and Neutrophil Oxidative Burst Index (NOBI) and normal IgG, IgM and IgA level. Lymphocyte proliferation was noted to be normal. Immunophenotyping showed normal percentages of CD3, CD4, CD8, CD19, CD4:CD8 ratio and NK cells. He was negative for HLA-B27. The following autoantibodies were noted to be negative: Anti-Nuclear Antibody (ANA), Anti-Smooth Muscle Antibody (Anti-SMA), Anti-Parietal Cell Antibody, Anti-Cardiolipins IgM and IgG, and Rheumatoid Factor. *IL10, IL10RA* and *IL10RB* genes were sequenced and no mutations were identified, and STAT3 phosphorylation was noted to be normal after stimulation of PBMCs with IL-10. His most recent immunological work up showed a normal Neutrophil Oxidative Burst Index (NOBI) and a normal immunophenotyping analysis of lymphocytes. Functional studies demonstrated abnormal TNFα response to L18-MDP stimulation (Figure S8). Because of this abnormal MDP response, the patient had directed sequencing of XIAP on 4 separate occasions at 2 institutions and no disease causing mutations were identified.

Patient 3: Patient 3 presented at age 7 years with severe hypoalbuminemia, bloody diarrhea and weight loss of a few weeks duration. Previously she had an unremarkable medical history and was born to consanguineous parents. She had been unwell for approximately 1 year prior to presentation and found to have severe anemia requiring a transfusion and elevated acute phase reactants. She presented with pericarditis and was admitted to the ICU. After initiating steroids, she responded initially. Her prior medical history was unremarkable and included only reactive airway disease. There was a strong family history of Crohn's disease in both her mother and maternal aunt. Her initial colonoscopy was limited due to severity but showed continuous colitis with cobble stoning and friability. Pathology showed chronic inflammation of the colon with partial villous blunting of the duodenal villi.

She continued on steroids but continued to be steroid dependent despite azathioprine. She was noted to develop a rectovaginal fistula, along with perianal disease. Due to continued disease activity, perianal disease and steroid dependence, infliximab was initiated with no significant improvement. She had repeated endoscopic evaluation showed pseudopolyps and discontinuous disease of the colon. Her terminal ileum showed edema and her perianal disease required multiple interventions using Seton placement and skin graft surgery.

Due to continued disease and lack of response, she subsequently underwent diversion ileostomy, followed by total proctocolectomy and abdominal perineal resection. Pathology of the resected specimen noted granulomas and inflammation involving the terminal ileum. Subsequent biopsies from colonoscopies done after surgery have all shown granulomas and mild patchy chronic colitis. She was started on Adalimumab therapy.

Despite diversion and second line anti-TNF therapy, she continued to have perianal disease with partial response. She also developed iritis and erythema nodosum. At last follow-up, she had transitioned to adult care while on azathioprine and steroid and antibiotic therapy. For her immunological workup, she was noted to have a normal level of IgG, IgA, and IgM. NOBI was repeatedly found to be normal. She did not have mutations in *IL10RA/B, IL10*, or *NEMO.* The patients had a c:109 del C, p: P37QfsX32 mutation in *XIAP* but is female and a heterozygote carrier. As the variants in *TRIM22* are also found in databases it is possible that the *XIAP* variant may contribute to disease in this patient. However, Patient 3 has transferred to adult care and no longer consented to any further immunological testing. Therefore no MDP functional studies were carried out.

Supplemental Tables

S1A) *Clinical Features*

Patient #	Age of Onset of Symptoms	Gender	Consanguinity	Clinical Features	Ethnicity/ History of IBD
1	8 days	Female	Yes	Diarrhea, rectal bleeding, perianal disease, growth failure, weight loss, epithelial granuloma	Lebanese No family history of IBD
2	< 3 months	Male	No	Severe growth failure, perianal disease, fever, petechiae, hepatomegally, diarrhea, polyarthritis involving mainly large joints.	Jamaican Strong maternal family history of Crohn's Disease
3	~ 6 years and presented at 7 years	Female	No	Diarrhea, abdominal pains, weight loss, diffuse edema of lower extremities, significant anemia.	Caucasian Strong maternal family history of Crohn's Disease

S1B) *Genetic Features*

Patient #	SNP	Exon	Variant Position			MAF	Prediction			
			Genomic (GrCh37.p13)	cDNA	Protein		Polyphen2 Rank Score	SIFT Rank Score	GERP++ Rank Score	PhyloP Rank Score
1	rs187416296	7	g.5730705C>T	c.1324C>T	p.Arg442Cys	0.0041	Probably Damaging (0.87578)	Damaging (0.90636)	1.68	0.36288
2	rs61735273	2	g.5719756C>T	c.731C>T	p.Ser244Leu	0.0035	Probably Damaging (0.8513)	Damaging (0.90636)	0.40419	0.77407
	rs200924168	3	g.5718503G>C	c.449G>C	p. Arg150Thr	0.0044	Possibly Damaging (0.47786)	Tolerated (0.3317)	0.01094	0.00845
3	rs12364019	7	g.5730343G>A	c.962G>A	p.Arg321Lys	0.015	Probably Damaging (0.83275)	Damaging (0.70945)	0.32553	0.34637

Table S1. Clinical (A) and Genetic Features (B) of Patients with TRIM22.
MAF minor allelic frequency based on 1000 Genomes and 6503 healthy individuals genotyped in the NHLBI Exome Sequencing Project (http://evs.gs.washington.edu). The variant prediction are based Polyphen2[18], SIFT (http://sift.jcvi.org), GERP++ (http://mendel.stanford.edu/SidowLab/downloads/gerp/), and PhyloP (http://ccg.vital-it.ch/mga/hg19/phylop/phylop.html).

Position	Chromosome	Position	Identifier	Reference	Gene Name	Parent	Parent	Patient
1:76226952-SNV	1	76226952	?	T	ACADM, DLSTP1	C_T	C_T	C_C
3:111793206-SNV	3	111793206	?	C	TMPRSS7	C_T	C_T	T_T
3:112648127-Del	3	112648127	rs4596117; ?	T	CD200R1	-_T	G_T	G_G
6:132206095-SNV	6	132206095	?	C	ENPP1	A_C	A_C	A_A
7:21698453-SNV	7	21698453	?	A	DNAH11	A_G	A_G	G_G
7:21781702-SNV	7	21781702	?	A	DNAH11	A_G	A_G	G_G
7:91623968-SNV	7	91623968	?	G	AKAP9	A_G	A_G	A_A
10:75442543-SNV	10	75442543	?	C	AGAP5	C_T	C_T	T_T
11:5730705-SNV	11	5730705	?	C	TRIM22	C_T	C_T	T_T
11:73796902-SNV	11	73796902	rs78878933	T	C2CD3	C_T	C_T	C_C
11:78419504-SNV	11	78419504	?	G	ODZ4	A_G	A_G	A_A
19:15730499-Ins	19	15730499	rs55848814	-	CYP4F8	-_C	-_C	C_C

Table S2. Autosomal Recessive Variants Identified by WES in Patient 1.

Table S3: VEO Genes
See excel sheet

Table S4. VEOIBD Key Drivers
See excel sheet

Table S5. IIBDGC GWAS Enrichment in TRIM22 Locus
See excel sheet.

Table S6. IIBDGC GWAS Enrichment in TRIM22 eQTL Enrichment
See excel sheet

Table S7. eQTL Pathway Enrichment
See excel sheet

Table S8. Crohn's GWAS Enriched Blood eQTL Overlap with the VEO Network

Table S9. Annotation of 179 VEO Network
See excel sheet

Table S10. Functional Categories of Genes in the TRIM22 Sub network

Table S11. Inflamed Sigmoid and Rectum Key Drivers

TRIM22 Levels at Intestine Site	CDAI Correlation	CDAI P Value	Baseline_CRP Correlation	Baseline_CRP P Value	Baseline_Fecal Calprotectin Correlation	Baseline_Fecal Calprotectin P Value	# of samples
Ileum	-1.23E-01	9.34E-02	4.41E-02	5.53E-01	4.15E-02	5.76E-01	193
Ascending	-5.39E-02	5.57E-01	1.64E-01	7.52E-02	2.45E-01	6.93E-03*	128
Transverse	1.70E-01	5.53E-02	1.74E-01	5.30E-02	3.66E-01	2.26E-05*	134
Descending	4.84E-02	6.49E-01	1.89E-01	7.67E-02	5.50E-01	1.40E-08*	96
Sigmoid	-1.52E-01	2.05E-01	8.79E-02	4.63E-01	4.96E-01	9.43E-06*	75
Rectum	-5.02E-02	5.09E-01	1.85E-01	1.53E-02	3.85E-01	1.46E-07*	184
Total	-2.65E-03	9.41E-01	1.26E-01	5.21E-04*	2.86E-01	6.54E-16*	810

Table S12. Correlations of the Expression of TRIM22 to the Clinical Response Characteristics Stratified by Distinct Intestine Anatomy Sites (Includes Both Inflamed and Non Inflamed Samples).

CDAI	Rho	P value
TRIM22	0.0829	0.0203

Table S13. Correlation of the Expression of TRIM22 in blood to CDAI

Supplemental Figures

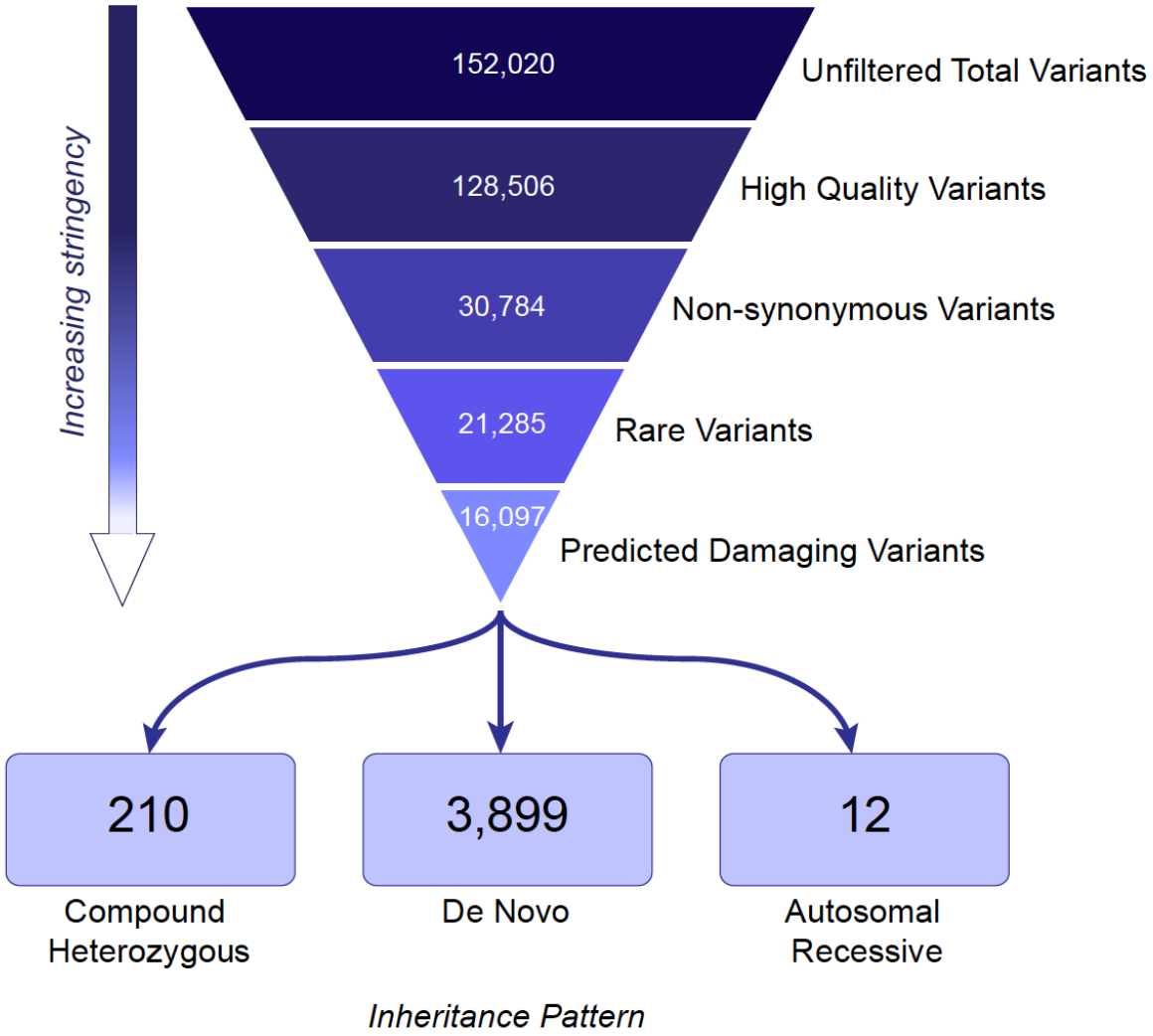

Figure S1: Variant Identification Pipeline for WES of Patient 1.

Whole exome sequencing identified 152,020 exonic variants in Patient 1. Eliminating low-quality and synonymous variants further refined the WES variant set. To isolated potential causative variants, only rare and predicated damaging (by dbNSFP) variants were included in inheritance analysis. Variants identified according to each inheritance model are shown.

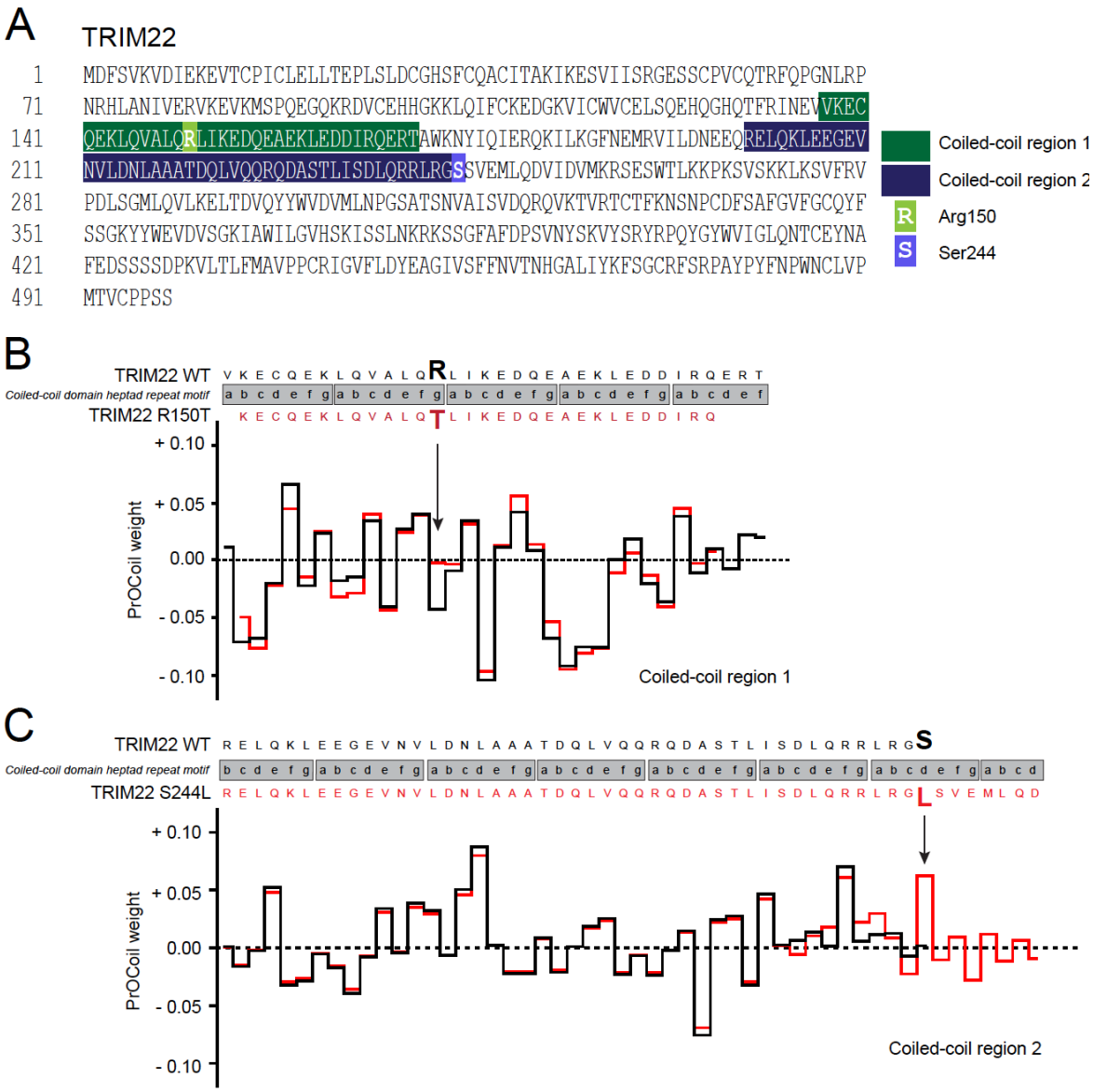

Figure S2: Heterozygous TRIM22 Variants R150T and S244L Occur in the Coiled-coil Domain and May Affect Domain Oligomerization.

A) Protein sequence for TRIM22 indicating the position of the two coiled-coil regions termed region 1 (green) and region 2 (purple) including the position of R150 and S244.

B, C) PrOCoil analysis of coiled coil region 1 (B) and region 2 (C) for TRIM22 with the corresponding variants reveals potential alterations in domain oligomerization patterns. PrOCoil evaluates the relative weighted contribution of each amino acid to the oligomeric character of the coiled-coil domain. The introduction of the R150T and S244L variants alter the weighted effect of positions near the site of variant. These alterations have potential to impact the ability of the coiled-coil domain to fold correctly.

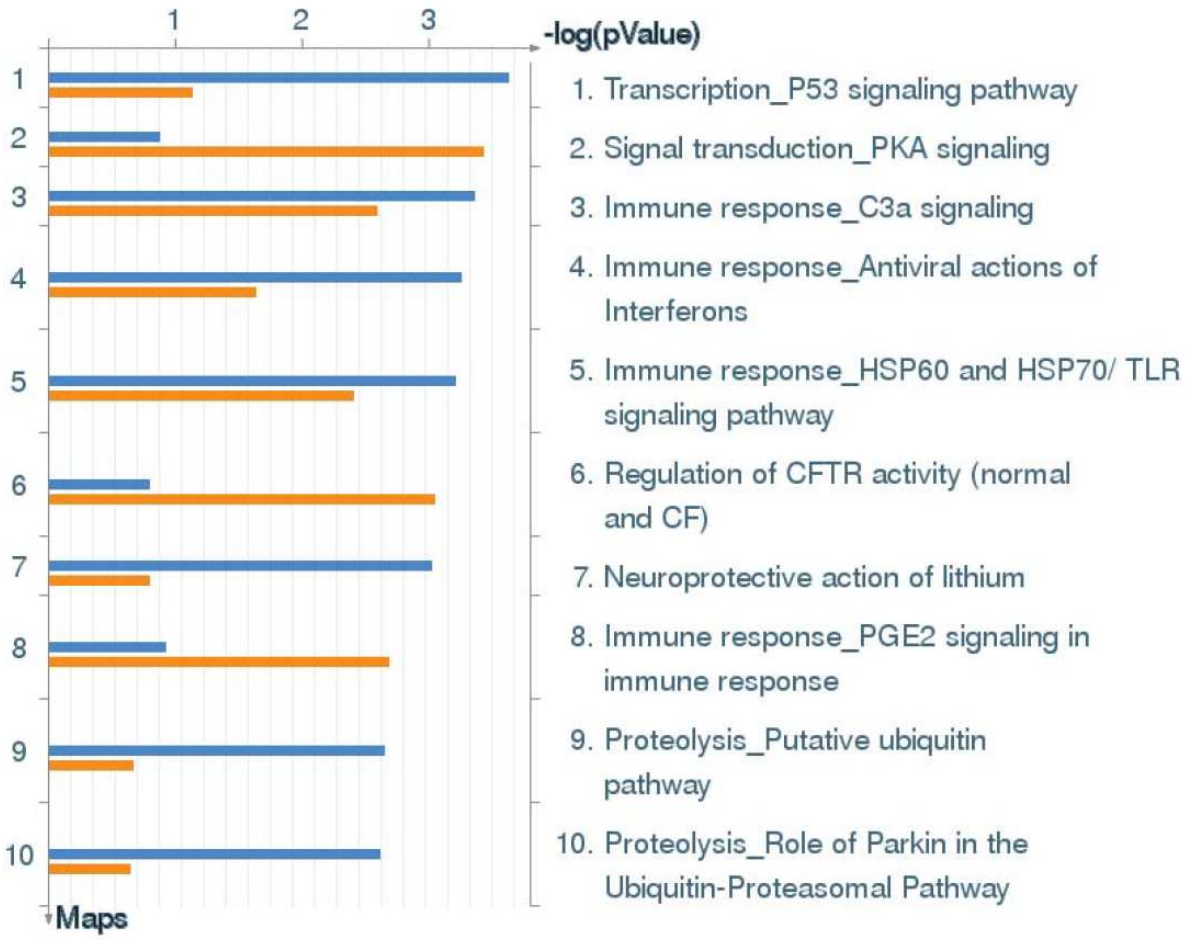

Figure S3: Blood and Intestine Derived eQTLs:
Gene Set Enrichment Analysis of Genes Controlled by IBD SNPs (Metacore)
See Table S7 for genes in pathway.

Top enriched gene sets among genes controlled by IBD SNPs: NHGRI catalog entries for IBD, UC and CD, plus all WTCCC IBD GWAS SNPs with p-value ≤ 0.001. 362 genes showed IBD SNP regulation in the blood, 98 in the intestine (56 genes were shared between the two tissues). Log10 p-value of enrichment on the horizontal axis: intestine (blue bar) and blood (orange bar).

Different Gene Set database categories are reported in each panel: TRIM22 Pathways: See below
1. Transcription P53 signaling (TRIM22 is a P53 target gene)
4. Immune response: Antiviral actions of interferons
9. Ubiquitin Pathway

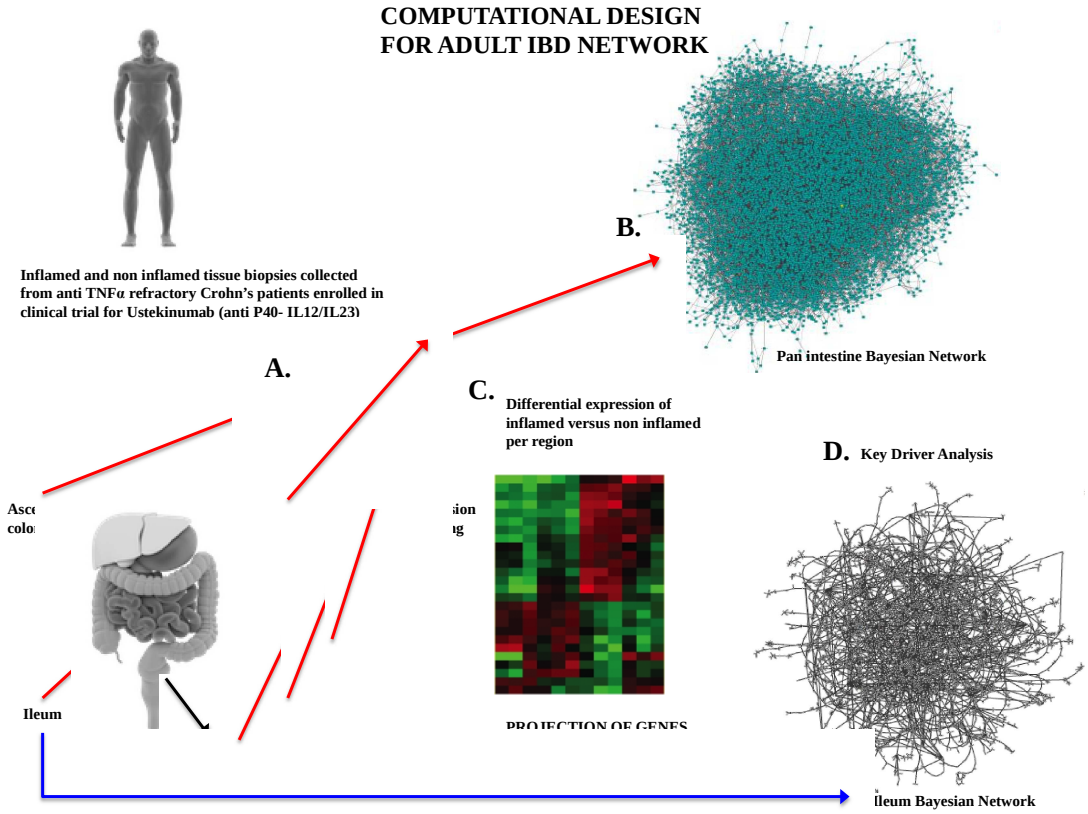

Figure S4: Computational Design.

A) Inflamed and non inflamed tissue biopsies were collected from anti TNFα refractory Crohn's patients enrolled in clinical trial for ustekinumab (anti P40- IL12/IL23).

B) Bayesian pan intestine network was constructed from microarray expression profiling on biopsies collected from various regions of the intestine.

C) Differential expression was performed on inflamed vs. non-inflamed for each region of the intestine collected.

D) Differential expression signatures of genes up regulated in inflamed sigmoid and inflamed rectum were projected on Bayesian ileum network for key driver analysis.

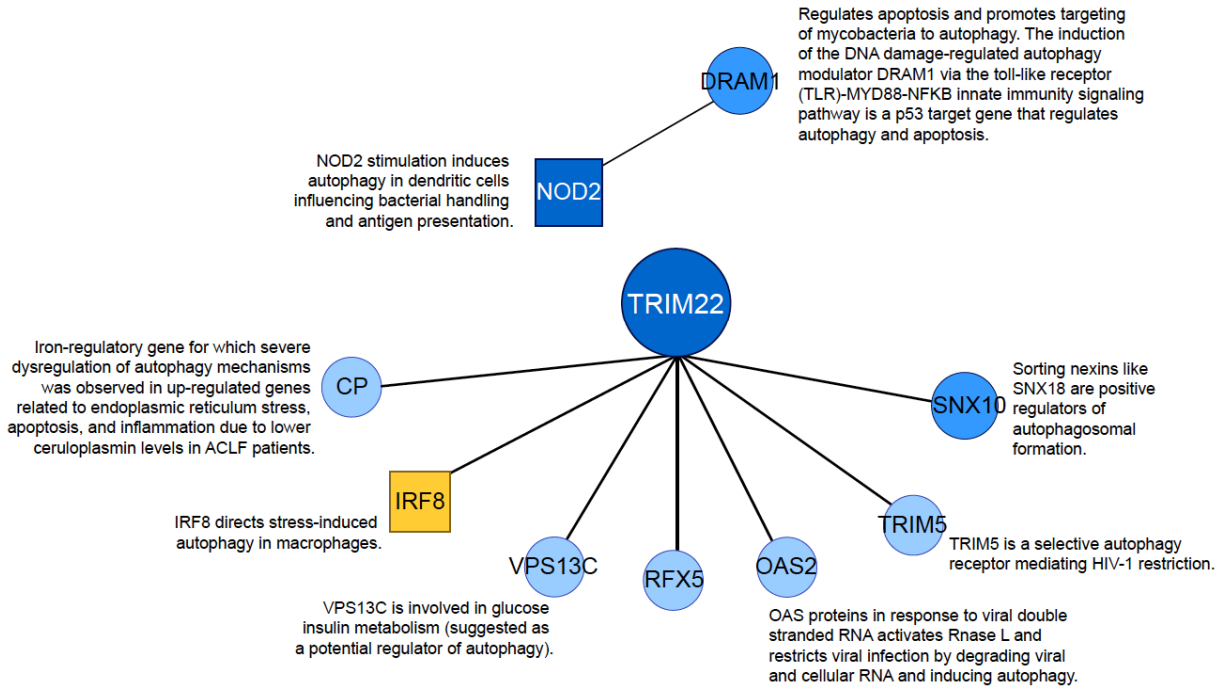

Figure S5: First Neighbors of TRIM22 and NOD2 in VEOIBD Intestine Network.

Genes within one path of TRIM22 in the VEOIBD RISK network have putative functional roles in autophagy.

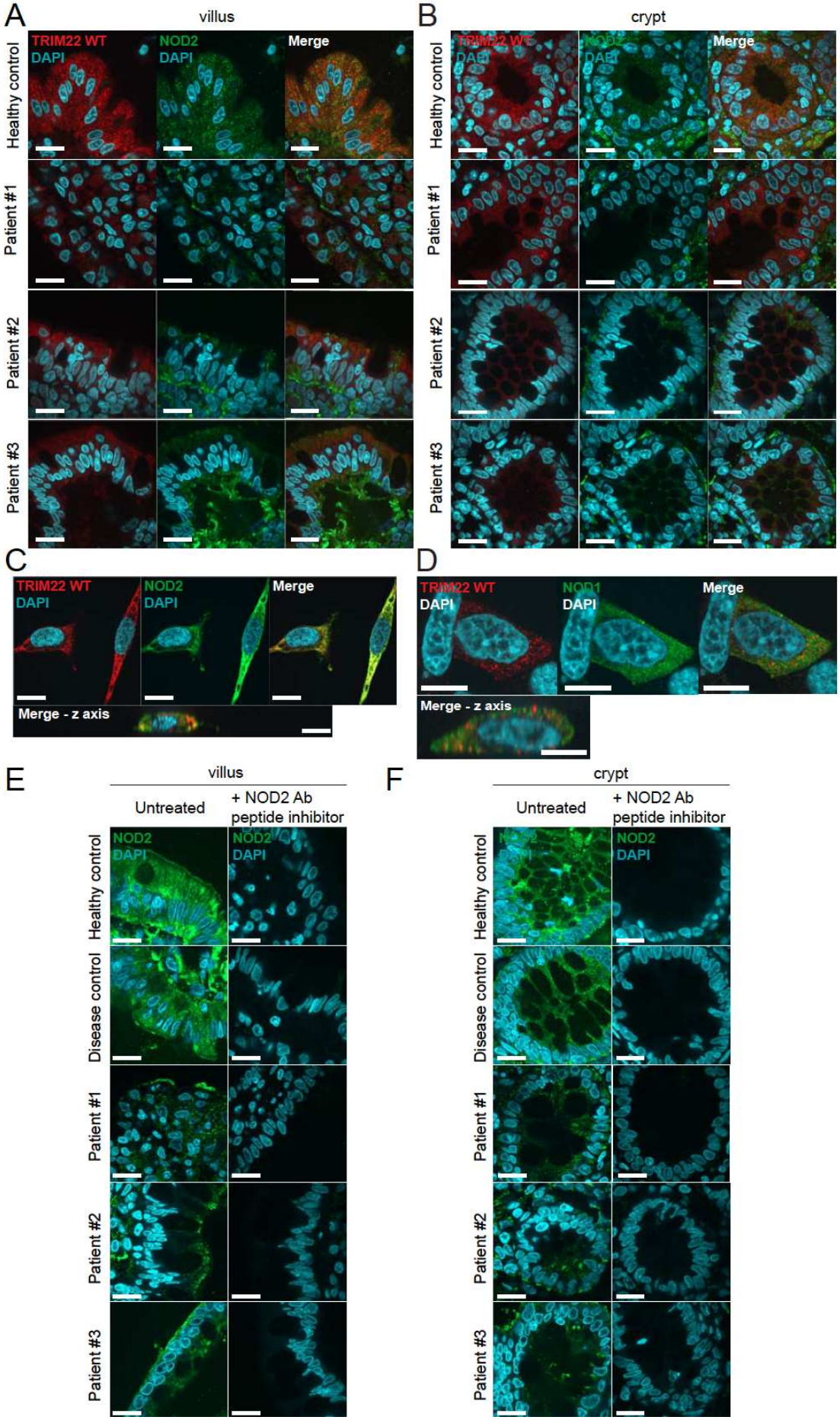
A
villus
TRIM22 WT
DAPI
NOD2
DAPI
Merge
Healthy control
Patient #1
Patient #2
Patient #3
B
crypt
TRIM22 WT
DAPI
Merge
Healthy control
Patient #1
Patient #2
Patient #3
C
TRIM22 WT
DAPI
NOD2
DAPI
Merge
Merge - z axis
D
TRIM22 WT
DAPI
NOD1
DAPI
Merge
Merge - z axis
E
villus
Untreated
+ NOD2 Ab
peptide inhibitor
NOD2
DAPI
Healthy control
Disease control
Patient #1
Patient #2
Patient #3
F
crypt
Untreated
+ NOD2 Ab
peptide inhibitor
NOD2
DAPI
Healthy control
Disease control
Patient #1
Patient #2
Patient #3

Figure S6: TRIM22 and NOD2 Co-localize in Healthy Controls and Disrupted in Patient Tissue Sections.

A, B) *Immunofluorescence analysis of TRIM22 and NOD2 in colonic biopsy samples from Healthy Controls and Patients.*
TRIM22 (red) and NOD2 (green) localization was analyzed in the villus (A) and crypts (B) of both healthy controls and Patients 1-3. TRIM22 and NOD2 colocalization was observed in the both the villus and crypts of the healthy control biopsy samples. Both TRIM22 and NOD2 expression and colocalization were reduced in the patient biopsy samples Scale bars represent10 μm.

C) *Exogenous TRIM22 co-localize with Exogenous NOD2*.
HEK293T cells seeded on coverslips were co-transfected with FLAG-TRIM22 and HA-NOD2. TRIM22 (red) and NOD2 (green) immunostaining show strong cytoplasmic colocalization. Scale bars represent 10μm.

D) *TRIM22 does not co-localize with NOD1*.
To evaluate the specificity of the observed TRIM22 and NOD2 co-localization, immunofluorescence microscopy was performed on HEK293T cells transiently expressing FLAG-TRIM22 and HA-NOD1, a NOD family member that does not interact with TRIM22. TRIM22 (red) and NOD1 (green) staining did not show significant overlap. Scale bars represent 10μm.

E, F) *Peptide inhibition of NOD2 in colonic biopsy samples of Healthy Controls and Patients.*
To demonstrate NOD2 antibody specificity, endogenous NOD2 immunostaining was performed on health and disease control biopsy samples as well as Patients 1-3 in the presence or absence of a NOD2 antibody peptide inhibitor. Without peptide incubation, NOD2 showed a cytoplasmic expression in healthy controls and disease controls, and is reduced in the patients. The specific NOD2 peptide is blocking the antigen-antibody binding and therefore no staining is detected when the peptide is added concurrently.

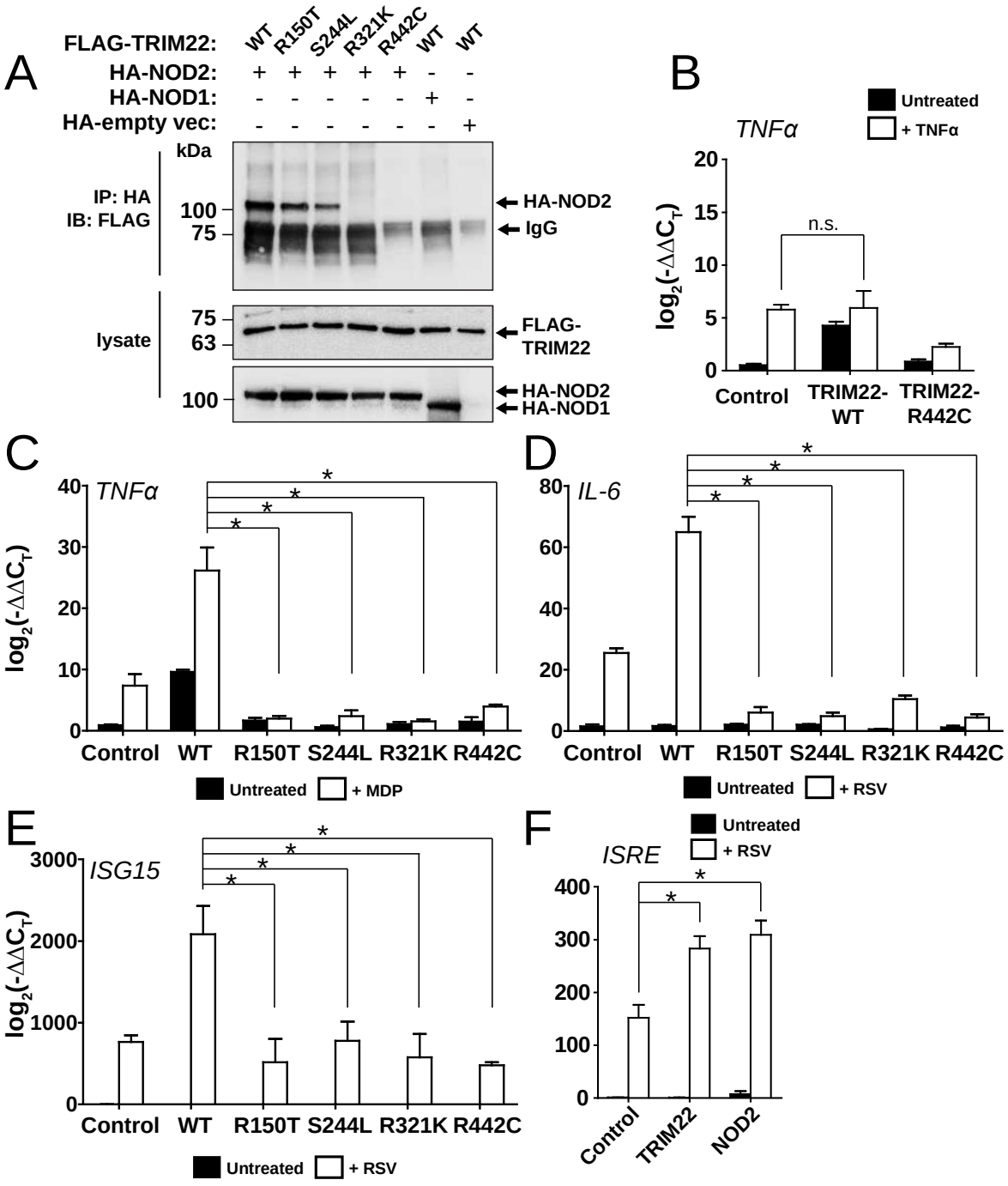

Figure S7: TRIM22 Variants and shRNA Abrogate NOD2 Signaling.

A) *NOD2 co-immunoprecipitates TRIM22 from in vitro cell lysates after transient co-expression*. HEK293T cells were transfected with HA-epitope tagged NOD2 and either wild type (WT) or mutant (R150T, S244L, R321K, R442C) FLAG-epitope tagged TRIM22 constructs. Twenty-four hours post-transfection, cells were lysed and NOD2 was immunoprecipitated with anti-HA antibody. Western blotting identified bound proteins. WT-TRIM22 interacted with and pulled-down NOD2; however, mutant TRIM22 showed reduced or absent NOD2 binding. NOD1, which does not interact with TRIM22, and an empty vector construct were included as negative controls. All lucerifase assay and Western blotting experiments were carried out in triplicate independent experiments and blots are representative.

B) *TRIM22 overexpression has no effect on TNFα mRNA levels following stimulation by TNFα.* HCT116 cells were transiently transfected with control (empty vector), TRIM22-WT, or TRIM22-R442C plasmids. Twenty-four hours post-transfection, cells were stimulated for 18 hr with TNFα (20 ng/mL). mRNA of TNFα were assessed by Q-PCR. No significant increase in TNFα mRNA was observed following TNFα stimulation of cells overexpressing TRIM22.

C, D, E) *TRIM22 mutants reduce mRNA level of genes downstream of the NOD2 signalling.* HCT116 cells were transiently co-transfected with NOD2 and TRIM22-WT or TRIM22 mutants (R150T, S244L, R321K, R442C). Twenty-four hours post-transfection, cells were stimulated with MDP (10 µg/mL) (C) or RSV (0.1 µg) (D, E) for 18 hr and then qPCR were performed. Cells transfected with TRIM22 mutants showed significantly reduced expression of *TNFα* (C), *IL-6* (D), and *ISG15* (E) (*$p < 0.001$ after Bonferroni post-hoc testing).

F) *Overexpression of TRIM22 increases ISRE activation.* HEK293T cells were transiently transfected with control (empty vector), TRIM22, or NOD2. ISRE reporter activation was evaluated by luciferase assay following stimulation with respiratory syncytial virus (RSV) (0.1 µg). TRIM22 overexpression significantly increased ISRE reporter activation compared to empty vector control (*$p<0.001$ after Bonferroni post-hoc testing). All experiments were carried out in triplicate, independent experiments.

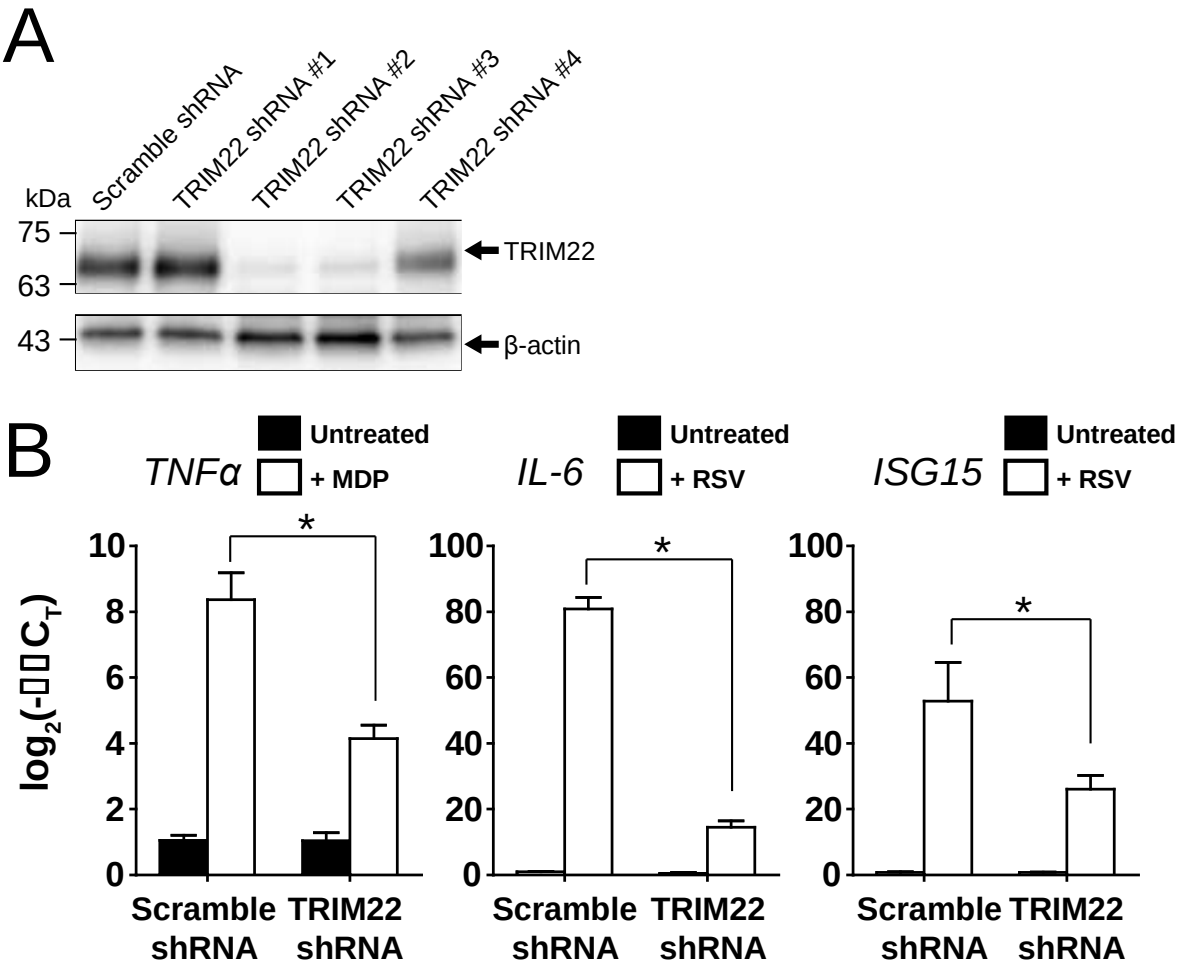

Figure S8: TRIM22 shRNA Knockdown.

A) To demonstrate the degree of knockdown present in cells expressing TRIM22 shRNA, HEK293T cells were transiently transfected with control (scramble) or various TRIM22 shRNA clones for 48 hours. Western blotting analysis was performed using anti-TRIM22 antibodies with β-actin staining as a loading control.

B) *Knockdown of TRIM22 reduces mRNA level of genes downstream of the NOD2.* mRNA of *TNFα*, *IL-6*, and *ISG15* were assessed by qPCR in HT29 cells stably transduced with control (scramble) or TRIM22 shRNA following stimulation by MDP (10 μg/mL) or respiratory syncytial virus (RSV) (0.1 μg). (*$p<0.001$ after Bonferroni post-hoc testing).

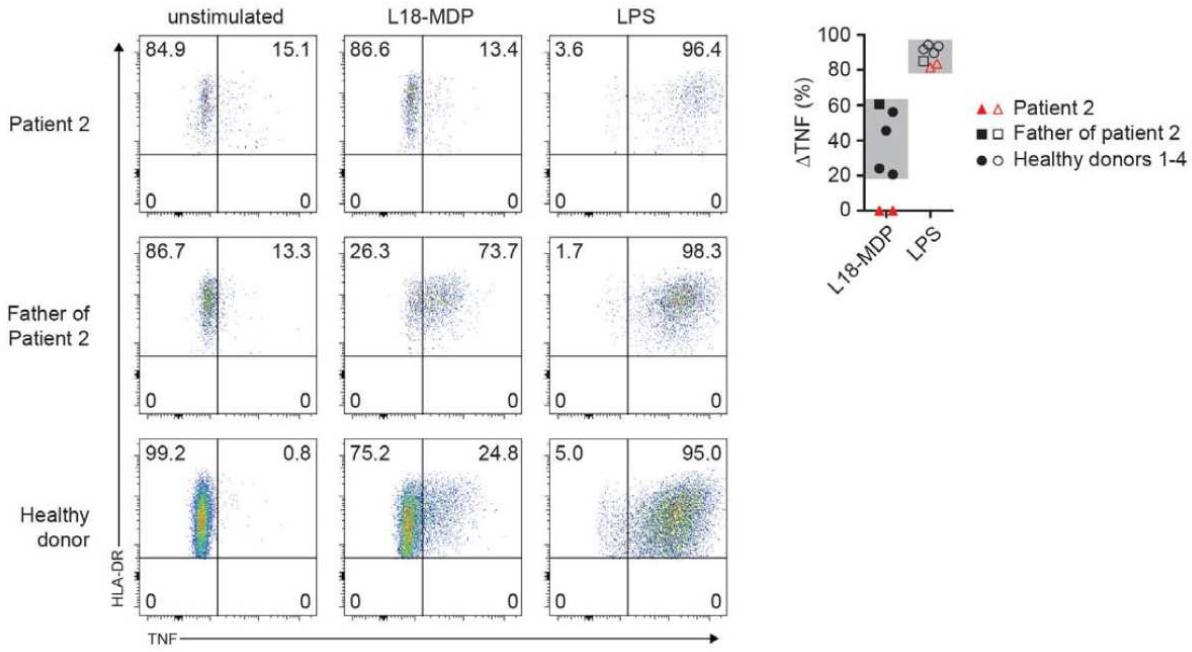

Figure S9: TRIM22 Variants Abrogates NOD2 Signaling in Patient 2 with Coiled-coil Variants.

Representative FACS blots and quantification of TNFα production in monocytes following stimulation with NOD2 and TLR4 ligand. Monocytes obtained from Patient 2 did not generate TNFα production in monocytes following stimulation with NOD2 and TLR4 ligand. Monocytes obtained from patient in response to L18-MDP stimulation but demonstrate normal reactivity to LPS. The patient's father and healthy donors are shown as controls. Monocytes are gated for single, live, CD14+, HLA-DR+ cells. ΔTNF (%) is determined by subtracting frequency of TNF-positive monocytes in stimulated from unstimulated conditions. Overnight travel of blood sample from Patient 2 and father of Patient 2 caused high baseline TNF without affecting results calculated as ΔTNF (%). Grey background indicates normal range. Similar results with patient 2 were obtained in two independent experiments performed ten months apart. Open symbols L18-MDP stimulation, closed symbols LPS stimulation. Similar results were not obtained from Patient 1 and Patient 3 was not tested as she did not consent to further testing.

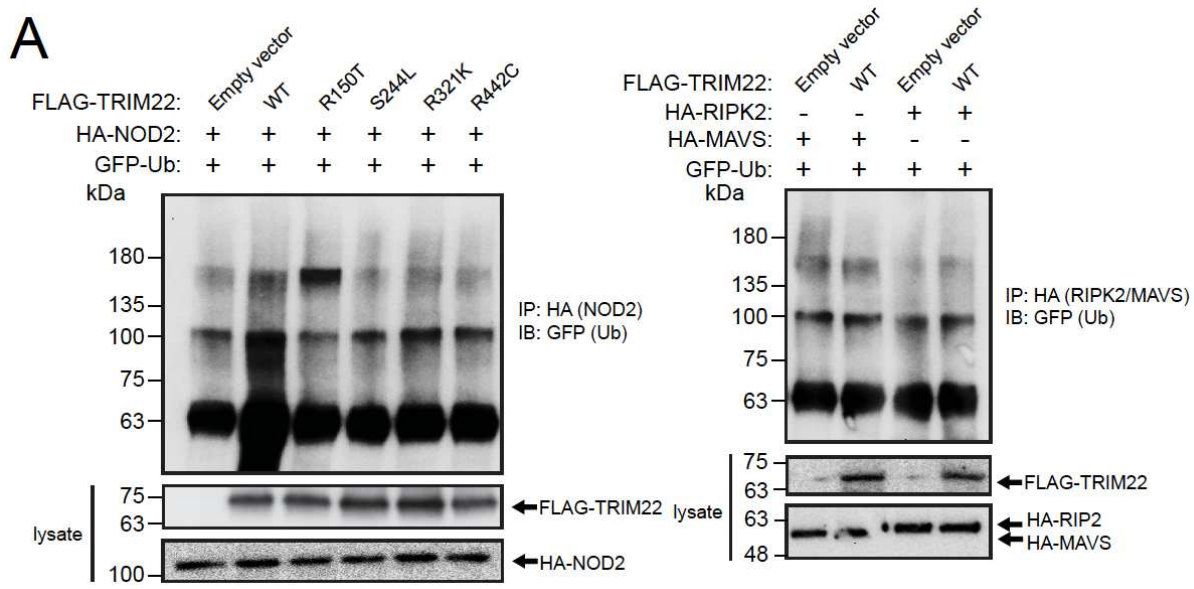

Figure S10: TRIM22 Directly Mediates the Polyubiquitination of NOD2 but not MAVS or RIPK2.

A) *Wildtype TRIM22 enhances polyubiquitination of NOD2 in HEK293 cells.*
HEK293 cells were transiently co-transfected with HA-NOD2, GFP-ubiquitin, and either wildtype (WT) or variant (R150T, S244L, R321L or R442C) FLAG-TRIM22. Following cell lysis, NOD2 was immunoprecipitated using anti-HA antibody bound to Protein G-Sepharose and NOD2 ubiquitination was observed by GFP immunoblotting. Co-transfection with WT-TRIM22 increased NOD2 ubiquitination that was lost in cells transfected with the TRIM22 variants.

B) *TRIM22 does not mediate the ubiquitination of MAVS or RIPK2.*
To determine if TRIM22 also regulates downstream NOD2 signaling modulators, HEK23T cells were co-transfected with FLAG-TRIM22, GFP-ubiquitin, and either HA-MAVS or HA-RIPK2. Twenty-four hours post-transfection, cells were lysed followed by immunoprecipitation of MAVS or RIPK2 using anti-HA-agarose. Immunoblotting for GFP-ubiquitin demonstrated no significant increase compared to empty TRIM22 vector controls. All experiments were carried out in triplicate independent experiments and blots are representative.

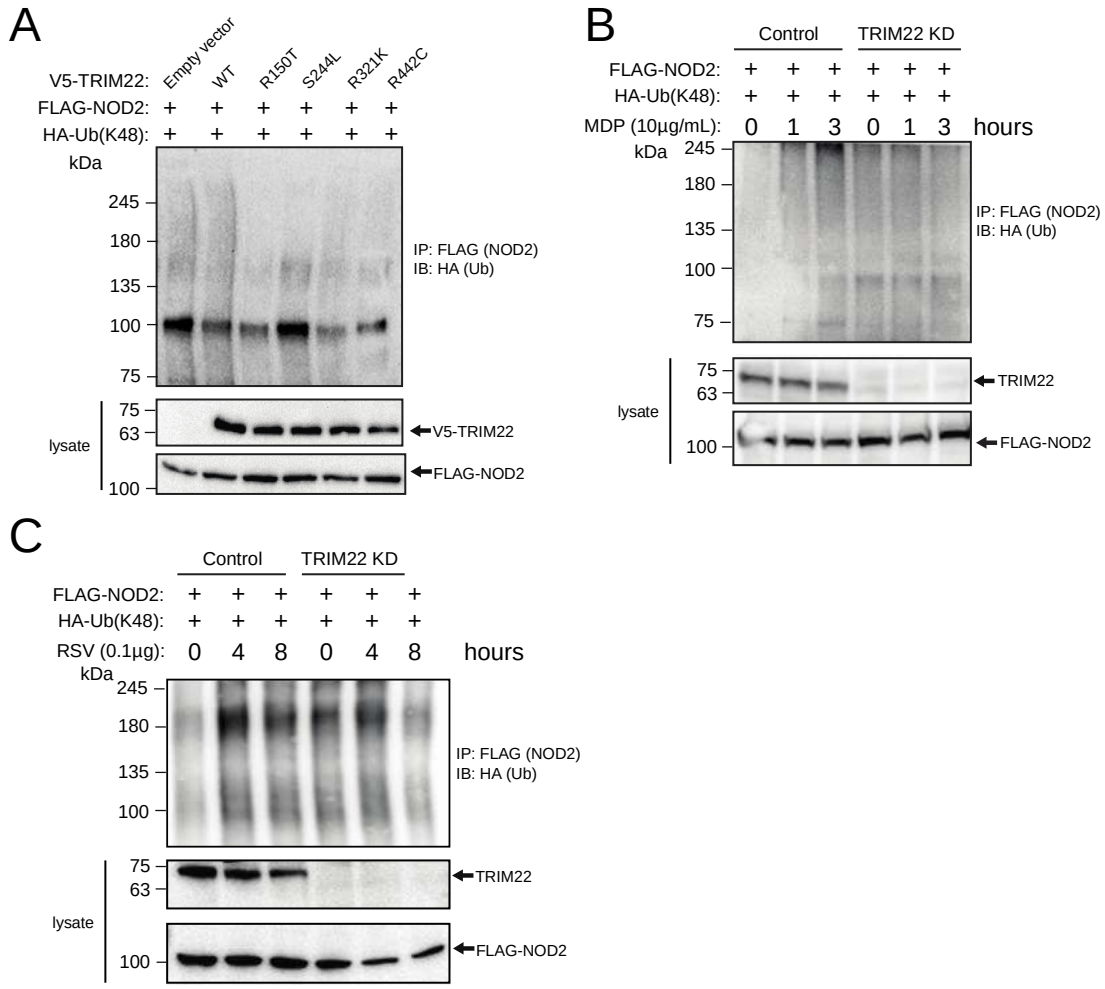

Figure S11: TRIM22 Does Not Mediate K48-linked Polyubiquitination of NOD2.

A) *TRIM22 does not mediate K48-specific polyubiquitination of NOD2.*
HEK293T cells were transiently co-transfected with FLAG-NOD2, HA-(K48-specific) ubiquitin, and either wildtype (WT) or variant (R150T, S244L, R321K, or R442C) V5-TRIM22. Twenty-four hours post-transfection, cells were lysed and NOD2 was immunoprecipitation with anti-FLAG-agarose. Immunoblotting for HA-tagged ubiquitin demonstrated no significant increase in cells transfected with WT-TRIM22 compared to empty vectors controls. Likewise, TRIM22 variants did not show significant K48-ubiquitin staining.

B, C) *TRIM22-shRNA does not reduce MDP and RSV induced K48-linked polyubiquitination of NOD2.*
HEK293T cells stably transduced with control (scramble) or TRIM22 shRNA were transfected with a HA-tagged K48-specific ubiquitin construct and FLAG-NOD2. Forty-eight hours post transfection, cell lysates were stimulated with MDP (B) or RSV (C) for the indicated time points followed by cell lysis and immunoprecipitation of NOD2 by anti-FLAG-agarose. In both control

and TRIM22 knockdown cells, stimulation did not result in increased NOD2 K48-specific poly-ubiquitination. Western blotting experiments were carried out in triplicate, independent experiments.

References

1. Sandborn WJ, Gasink C, Gao LL, et al. Ustekinumab induction and maintenance therapy in refractory Crohn's disease. The New England journal of medicine 2012;367:1519-28.
2. Madigan DaY, J. Bayesian graphical models for discrete data. International Statistical Review 1995;63:215-232.
3. Schwarz G. Estimating the dimension of a model. Annals of Statistics 1978;6:461-464.
4. Zhu J, Lum PY, Lamb J, et al. An integrative genomics approach to the reconstruction of gene networks in segregating populations. Cytogenet Genome Res 2004;105:363-74.
5. Schadt EE, Molony C, Chudin E, et al. Mapping the genetic architecture of gene expression in human liver. PLoS Biol 2008;6:e107.
6. Zhu J, Wiener MC, Zhang C, et al. Increasing the power to detect causal associations by combining genotypic and expression data in segregating populations. PLoS Comput Biol 2007;3:e69.
7. Zhu J, Zhang B, Smith EN, et al. Integrating large-scale functional genomic data to dissect the complexity of yeast regulatory networks. Nat Genet 2008;40:854-61.
8. Zhu J, Wiener MC, Zhang C, et al. Increasing the power to detect causal associations by combining genotypic and expression data in segregating populations. PLoS Comput Biol. 2007;3:e69. .
9. Zhang B, Horvath S. A general framework for weighted gene co-expression network analysis. Stat Appl Genet Mol Biol 2005;4:Article17.
10. Ravasz E, Somera AL, Mongru DA, et al. Hierarchical organization of modularity in metabolic networks. Science 2002;297:1551-5.
11. Langfelder P, Zhang B, Horvath S. Defining clusters from a hierarchical cluster tree: the Dynamic Tree Cut library for R. Bioinformatics 2007.
12. Zhang B, Gaiteri C, Bodea L-G, et al. Integrated Systems Approach Identifies Genetic Nodes and Networks in Late-Onset Alzheimer's Disease. Cell 2013;153:707-720.
13. Tran LM, Zhang B, Zhang Z, et al. Inferring causal genomic alterations in breast cancer using gene expression data. BMC Syst Biol 2011;5:121.
14. Wang IM, Zhang B, Yang X, et al. Systems analysis of eleven rodent disease models reveals an inflammatome signature and key drivers. Mol Syst Biol 2012;8:594.
15. Yang X, Zhang B, Molony C, et al. Systematic genetic and genomic analysis of cytochrome P450 enzyme activities in human liver. Genome Res 2010;20:1020-36.
16. Tusher VG, Tibshirani R, Chu G. Significance analysis of microarrays applied to the ionizing radiation response. Proc Natl Acad Sci U S A 2001;98:5116-21.
17. Uhlig HH, Schwerd T, Koletzko S, et al. The Diagnostic Approach to Monogenic Very Early Onset Inflammatory Bowel Disease. Gastroenterology 2014.
18. Adzhubei IA, Schmidt S, Peshkin L, et al. A method and server for predicting damaging missense mutations. Nat Methods 2010;7:248-9.